Sedimentation record in the Konkan-Kerala basin: Implications for the evolution of the Western Ghats and the Western Indian passive margin

D. Campanile[1], C. G. Nambiar[2], P. Bishop[1], M. Widdowson[3] and R. Brown[1]

[1]*Department of Geographical and Earth Sciences, University of Glasgow, Glasgow G12 8QQ, U.K. (Daniel.campanile@ges.gla.ac.uk)*
[2]*Department of Marine Geology and Geophysics, Cochin University of Science and Technology, Cochin, India (nambiarcg@yahoo.com)*
[3] *Department of Earth Science, The Open University, Walton Hall, Milton Keynes, MK7 6AA, U.K. (m.widdowson@open.ac.uk)*

ABSTRACT

The Konkan and Kerala Basins constitute a major depocentre for sediment from the onshore hinterland of Western India and as such provide a valuable record of the timing and magnitude of Cenozoic denudation along the continental margin. This paper presents an analysis of sedimentation in the Konkan-Kerala basin, coupled with a mass balance study, and numerical modelling of flexural responses to onshore denudational unloading and offshore sediment loading in order to test competing conceptual models for the development of high-elevation passive margins. The Konkan-Kerala basin contains an estimated 109,000 km^3 of Cenozoic clastic sediment, a volume difficult to reconcile with the denudation of a downwarped rift flank onshore, and more consistent with denudation of an elevated rift flank. We infer from modelling of the isostatic response of the lithosphere to sediment loading offshore and denudation onshore infer that flexure is an important component in the development of the Western Indian Margin. There is evidence for two major pulses in sedimentation: an early phase in the Palaeocene, and a second beginning in the Pliocene. The Palaeocene increase in sedimentation can be interpreted in terms of a denudational response to the rifting between India and the Seychelles, whereas the mechanism responsible for the Pleistocene pulse is more enigmatic.

INTRODUCTION

Passive continental margins (PCMs) develop on the trailing edges of tectonic plates in response to continental rifting, sea floor spreading and ocean basin development (Kearey & Vine, 1996). The anatomy of PCMs is dependent on a range of factors, including the pre-rift topography, drainage network evolution, syn- and post- breakup, denudation, proximal basin development, climatic control on rock weathering, long-term sea level fluctuations, thermal evolution of the lithosphere and flexural properties of the lithosphere (Summerfield, 1991; Watts, 2001; Allen & Allen, 2005). Despite this range of factors controlling the evolution of any particular margin, the macro-geomorphology of high elevation PCMs of Gondwanan continents is remarkably consistent, comprising a low elevation coastal plain and an elevated interior plateau separated by an escarpment running parallel to the coastline (Ollier, 1982, 1985; Gilchrist & Summerfield, 1990).

Two broad groups of competing conceptual models have been developed to describe qualitatively the post-rift evolution of high elevation PCMs. These conceptual models are: escarpment retreat into a downwarped rift shoulder (King, 1967; Ollier & Pain, 1997) and escarpment development into an elevated rift shoulder (Gilchrist & Summerfield, 1990; Gilchrist *et al.*, 1994; Kooi & Beaumont, 1994; Tucker & Slingerland, 1994). These competing conceptual models differ fundamentally in the magnitude of denudation, and the volume of sediment deposited offshore. The downwarp model advocated by King (1967) and Ollier and Pain (1997) assumes that the lithosphere is flexurally rigid and, accordingly, postulates the removal of small amounts of crust at the coast increasing to a maxima at the escarpment (Fig. 1a and b). The magnitude of unroofing at the coast is so small that incomplete destruction of the downwarped surface occurs and isolated remnants are preserved (Fig 1b). By contrast, the elevated rift flank model and its associated mode of evolution is capable of generating much greater amounts of denudation by incorporating initial rift flank surface uplift and/or post-rift lithospheric flexure (Fig. 1d and e). Consequently, determining the mode of escarpment formation and the flexural response to escarpment formation is critical to improving our understanding of the evolution of, and subsequent sediment fluxes from, high elevation PCMs.

The rate of escarpment formation also exerts an important temporal control on denudation rates. Earlier conceptualisation of escarpment evolution requires formation by steady parallel retreat of the escarpment face between rifting/breakup and the present (King, 1955; Ollier, 1982, 1985; Gilchrist & Summerfield, 1990, 1994; Kooi & Beaumont, 1994; Tucker & Slingerland, 1994; Seidl *et al.*, 1996). However, the emerging view is that the development of these escarpments may be rapid and short-lived, with the escarpment reaching essentially its modern configuration in a relatively short time after rifting (Cockburn *et al.*, 2000; Matmon *et al.*, 2002; Persano *et al.*, 2002, 2005).

Western India exhibits many features common to elevated passive margins, but additionally includes a coast-parallel monocline clearly observed inland of Mumbai (Auden, 1949). Such coast-parallel monoclines have been used to support passive margin evolution by escarpment retreat into a downwarped rift flank (King, 1967; Ollier & Pain, 1997). The deformation of laterite surfaces developed on the Deccan lavas indicates protracted and ongoing post-rift lithospheric flexure, a response which can only be adequately explained by the downwarp hypothesis if the model is adapted (Widdowson & Cox, 1996; Widdowson, 1997; Widdowson & Mitchell, 1999) (fig 1c). Within the Deccan Volcanic Province (DVP) the margin displays a downwarped geometry but with 1-2 km of denudation across the coastal plain (Widdowson & Cox, 1996; Widdowson, 1997), magnitudes inconsistent with the King (1967) and, Ollier and Pain (1997) downwarp model.

Along strike, south of the DVP, the mode of escarpment development remains more elusive. Seaward cambering of laterites on the coastal plain (Widdowson & Gunnell, 1999) indicate that a modified Widdowson (1997) downwarp model may continue south of the Deccan. Further support for a modified Widdowson (1997) downwarp model is provided by numerical surface process models for the Western Indian margin where a downwarped geometry (with accompanying lithospheric flexure) can be generated (Gunnell & Fleitout, 1998, 2000). However, numerical surface process modelling incorporating initial rift flank uplift or an isostatic response to denudational unloading generates margin morphologies analogous to the elevated rift flank model (Gunnell & Fleitout, 1998, 2000). Apatite fission track thermochronometry (AFTT) has been employed to quantify the rate and timing of denudation on the margin (Kalaswad *et al.*, 1993; Gunnell *et al.*, 2003). AFT data from coastal areas were reset at the start of the Palaeocene indicate ca. 2-4 km of denudation. AFT data further inland were not reset, indicating much smaller magnitudes of denudation than at the coast. This pattern of denudation is more consistent with escarpment evolution into an elevated rift flank.

Denudation, sediment supply, and the resultant lithospheric flexural response are intrinsically linked, and the analysis of offshore sedimentation coupled with other methodologies such as AFT thermochronology and drainage basin development are valuable approaches for constraining landscape development on PCMs (e.g., Brown *et al.*, 1990; Rust & Summerfield, 1990; Pazzaglia & Gardner, 1994; Pazzaglia & Brandon, 1996) . However, most studies of the Western Indian margin have tended to focus on either the onshore post-rift denudational history, or the offshore depositional record, with only a few notable exceptions attempting to integrate both methodologies (Gunnell & Fleitout, 1998, 2000; Gunnell, 2001b). This paper presents an evaluation of the sedimentation history within the Konkan-Kerala basin in order to constrain the timing and magnitude of post-rift denudation for the adjacent onshore hinterland of the Western Ghats. Sediment mass balance analysis is then undertaken by placing the recompacted clastic volume of sediment onto a pre-defined area of the continental margin in order to determine the style of landscape development. Two competing conceptual models of escarpment evolution are tested: the downwarped rift flank model with no post-rift lithospheric flexure

(King, 1967; Ollier & Pain, 1997), and the elevated rift flank model. The analysis is further refined by modelling the isostatic flexural response of the lithosphere to sediment loading offshore and denudational unloading onshore to assess the role of flexural isostasy (if any) in the development of the margin.

REGIONAL GEOLOGY, TECTONICS & GEOMORPHOLOGY

The varied geology along the Western Indian passive margin can be generalized into several regions. The north (16° - 22°N) is characterised by the extensive Deccan flood basalts covering the margin as far south as Belgaum (Fig. 2). These sub-horizontal basalts lie unconformably on the crystalline basement, infilling and blanketing a pre-existing shield topography (Jerram & Widdowson, 2005). Our interest is the area south of the Deccan flood basalts (8° - 16°N), where the margin is composed of crystalline basement with Archaean basement gneiss and the younger metasediments of the Dharwar system forming the common rock types (Beckinsale *et al.*, 1980; Drury *et al.*, 1983; Naqvi & Rogers, 1987). The southern portion of the margin (i.e. south of 12°N) is composed almost entirely of Archaen charnokites, gneisses and granites (Naqvi & Rogers, 1987), though Tertiary sediments of limited extent occur locally, particularly along the coast of Kerala (Nair *et al.*, 2006). Proterozoic and Phanerozoic rocks are completely missing from the margin until the Deccan Traps are emplaced at the Cretaceous/Tertiary boundary.

The western continental margin of India and the adjacent oceanic regions are the result of a multi-stage rift history. Breakup of East Gondwana began in the early Jurassic ca. 180 Ma (Besse & Courtillot, 1988, 1991; Storey, 1995) followed by the separation of India-Madagascar (termed Greater India) from Africa ca 130-120 Ma (Reeves & de Wit, 2000). Greater India started to separated from Madagascar around 88 Ma (Storey, 1995), this separation being the first major rifting event to affect the Western Indian continental margin. Finally, a ridge jump in the nascent Indian Ocean resulted in the breakup of India and Seychelles at the end of the Late Cretaceous to form the current Western Indian margin (McKenzie & Sclater, 1971; Norton & Sclater, 1979; Naini & Talwani, 1982; Schlich, 1982). The emplacement of Deccan flood basalts at 65 Ma was contemporaneous with rifting of the Seychelles microcontinent (Norton & Sclater, 1979; Hooper, 1990), and was followed by rapid seafloor spreading creating the present day Arabian Sea (Courtillot *et al.*, 1986; Miles & Roest, 1993).

Western India has a well-defined escarpment, known as the Western Ghats or Sahyadri, paralleling the coast for 1500 km (Fig. 2). The Western Ghats are a shoulder-type escarpment (Matmon *et al.*, 2002) with the drainage divide near coincident with the top of the escarpment for most of its length. The average elevation of the escarpment is around 1200 m, and the escarpment is bounded on the landward side by plateaus of more than 800 m elevation along most of its length (Fig.2). The coastal plain on the seaward side has an average width of 60 km. There are four major embayments along the length of the escarpment, the largest being the Palghat Gap, which has generated an 80 km-wide breach of the escarpment (Fig. 2).

It is now well established that the Western Ghats are predominantly a denudational feature (Radhakrishna, 1967; Widdowson & Cox, 1996; Gunnell & Radhakrishna, 2001) and not a major fault scarp as previously postulated (Krishnan, 1960; Pascoe, 1964). There is a general lack of stratigraphic markers to constrain the escarpment's evolution and so palaeosurfaces have been used to reconstruct the denudational chronology of the margin (Radhakrishna, 1967; Vaidyanadhan, 1977; Radhakrishna, 1993; Gunnell, 1997; Widdowson, 1997)..

Post-rift surface uplift is certainly evident along the Western Indian margin (Radhakrishna, 1967; Widdowson & Cox, 1996; Gunnell, 2001a) but its causes remain unclear. Plume-related regional surface uplift and secondary mantle convection have been proposed (Cox, 1980; Thakur & Nagarajan,

1992) but these mechanisms are transient and so cannot explain persistent surface uplift and denudation long after the initial rifting event. Lithospheric necking, lithospheric delamination and magmatic underplating have also been invoked but such mechanisms also operate at shorter timescales (McKenzie, 1978; Cox, 1980). Other mechanisms that result in surface uplift persisting beyond the transient thermal effects associated with rifting include the impact of the Himalayan collision since the late Miocene (Gowd *et al.*, 1992), and flexural isostatic effects driven by denudational rebound onshore and sediment loading offshore (Widdowson & Cox, 1996; Widdowson, 1997; Gunnell & Fleitout, 1998, 2000).

OVERVIEW OF KONKAN-KERALA BASIN

The sedimentary basins adjoining the west coast of India include, from north to south, Kutch Offshore Basin, Cambay Basin, Saurashtra Basin, Surat Basin, Bombay Offshore Basin (collectively termed Northern Basins), the Konkan Basin and the Kerala Basin (Fig.2). The Northern Basins have a greater hydrocarbon potential than the Konkan and Kerala Basins, resulting in more intensive research and a better understanding of their sedimentation history (Mathur & Nair, 1993; Singh *et al.*, 1999). These data have aided our knowledge of the stratigraphy within the Konkan and Kerala Basins. For the purposes of this study, these Northern Basins have been excluded from the mass balance study due to their complexity in terms of multiple sediment sources. The Konkan and Kerala Basins are the focus of this study.

The Konkan and Kerala Basins are particularly useful in that they provide a sedimentary record since ca. 80 – 90Ma. The basins represent sag basin development on the stretched pre-Deccan continental basement during the rifting of India from Madagascar (Singh & Lal, 1993). Sedimentation in the Konkan and Kerala Basins is within coast parallel N-S trending grabens separated by local basements highs. Seismic profiles of the sediments indicate the presence of differential vertical movements as well as wrench faults, reverse faults and folds (Ghosh & Zutshi, 1989). Some of the faults may be basement controlled since the thinned crust underlying the sediments is characterized by a coast-parallel Precambrian grain (Kolla & Coumes, 1990; Subrahmanyam *et al.*, 1994, 1995).

The Vengurla Arch basement high is a natural barrier at 17° N latitude, and separates the Konkan Basin from basins to the north. Sediments north of the Vengurla Arch are not derived solely from the denudation of the Western Ghats and instead contain sediments from the Deccan basalt terrain, and the Cambay and Kutch grabens, as well as material from the Indus fan (Rao & Rao, 1995). The depositional history of these more northerly basins also differs from that of the Konkan and Kerala Basins, with the northern basins containing larger volumes of older (Mesozoic) sediments and rifted remnants of the extensive sub-aerial volcanism generated during Deccan eruptive episode. The Chagos-Laccadive Ridge does not form a complete barrier for sediment transport westwards; however, sediment thickness is reduced on the abyssal plain and is probably indicative of deep water pelagic processes or local sedimentation and not hinterland denudation. In effect, the inner shelf has been a closed sediment sink for the erosional products of the Western Ghats and hence provides an excellent record of onshore denudation.

The shelf sediments along the Western margin of India are strongly compartmentalised and show marked affinities along strike with their adjacent onshore areas. Thus, north of Goa, modern shelf sediments have a basaltic source, whereas south of Goa these sediments have a gneissic source (Rao & Rao, 1995; Rao & Wagle, 1997; Kessarkar*et al.*, 2003). Given this close relationship between the onshore geology and the offshore sediments, and lacking evidence to the contrary, we take it to be the case that there was little longshore transport of sediment in the Konkan and Kerala Basins during the Cenozoic. Although the the Konkan Basin is separated from the Kerala basin by the Tellicherry Arch basement high (fig. 2), both basins only source their sediments from the Western Ghats, and for the purposes of this study are grouped together here as the Konkan-Kerala basin.

The Upper Cretaceous early rift phase of sedimentation (i.e. Campanian) in the Konkan-Kerala basin is localized in narrow grabens in the south, west of Cochin. This sedimentation took place in a shallow continental setting (i.e., fan deltas, tidal flats and carbonate platforms) suggesting that a major part of the stretched portion of the crust on which the basin developed had remained above sea-level until at least pre-Santonian time (Singh & Lal, 1993). Upper Cretaceous sediments in the deepest wells of Konkan-Kerala basin overlie altered volcanic rocks. These basal volcanic rocks are undated, but outcrops of similar volcanic rocks nearer the coast (St. Mary Islands; Fig.2) have been dated as 85.6 Ma (Pande *et al.*, 2001), and hence are contemporaneous with Marion hot-spot magmatism (Joseph & Nambiar, 1996). Accordingly, basin initiation is likely to have occurred at 88 Ma, the time of India-Madagascar rifting and during the peak of Marion hotspot volcanism (Storey, 1995); nevertheless, the bulk of sediments in the Konkan-Kerala basin appear to have been deposited during the Cenozoic.

Passive subsidence in response to rifting between India and the Seychelles (fig. 3) began at the start of the Palaeocene and led to the development of an extensive marine basin containing sediments whose volumes are quantified in this study. Sediment isopach maps in the Konkan-Kerala basin indicate Cenozoic sediment thicknesses of up to 4 km (Rao & Srivastava, 1984). More typically, total sediment thickness ranges from 500 ms to 3500 ms (seismic two way travel times - TWT) averaging 1300 ms for the Konkan-Kerala Basins. The greatest accumulation occurs within coast-parallel graben structures that lie approximately 50-150 km offshore, thinning to less than 500 ms TWT over the Laccadive ridge which is a portion of the Chagos-Laccadive volcanic ridge produced by the Reunion hotspot (Subrahmanyam, 1995) (fig. 3). Data from eleven bore-holes (Singh & Lal, 1993; Gunnell, 2001b; Chaubey *et al.*, 2002; Rao *et al.*, 2002) may be combined into a generalized stratigraphy consisting of a thick carbonate accumulation (Eocene to Late Miocene) sandwiched between clastic-dominated sequences (Fig. 4). The major breaks in deposition/unconformities in the basin occurred in the Middle Paleocene, the Early Eocene and the Late Eocene-Early Oligocene; the Lower and Middle Miocene are also marked by unconformities (Singh & Lal, 1993).

Paleobathymetry estimates imply shallow depths (<100 m) for sedimentation within the Konkan-Kerala basin during the Upper Cretaceous (ca. 85 Ma) (Raju *et al.*, 1999). The basin became a major depocentre at 85-75 Ma when its depth increased to >200 m; however, uplift due to the onset of rifting led to a decrease in basin depth to near sea level from 65-60 Ma, and a period of non-deposition. Re-submergence then occurred in the Palaeocene/Eocene. The Konkan-Kerala basin is then interpreted to have followed a normal subsidence path for a rifted passive margin beginning with rapid initial subsidence in the Cretaceous, followed by slow thermal subsidence throughout the Cenozoic (Gombos *et al.*, 1995).

The development of a thick carbonate sequence in the Miocene throughout all the basins of the western continental margin of India has been linked to increased sea level and a drier and warmer climate in the Middle Miocene (Clift *et al.*, 2001; Molnar, 2004). However, during the late Miocene the Western Indian margin experienced a heavy influx of terrigeneous clastic sediments (Singh *et al.*, 1999). This phase of high sedimentation is associated with fracturing, shear zone movements, down-faulting and collapse of several parts of the shelf, and may be attributed to a change in the tectonic regime following the Himalayan collision (Ghosh & Zutshi, 1989). The markedly thicker sediments accumulated further northwest of the region are referred to as the Indus Fan where total sediment thickness reaches over 9km (Clift *et al.*, 2001), reflecting the very high sediment fluxes derived from the Himalaya (Fig. 2). Indus Fan sediments thin eastwards towards the Chagos-Laccadive Ridge and constitute an insignificant component of the Konkan-Kerala basin sediments (McHargue & Webb, 1986; Kolla & Coumes, 1990).

METHODS

Quantifying sediment volume

The data used here to document Cenozoic sedimentation in the Konkan Kerala Basin are derived from 11 commercial wells (Singh & Lal, 1993; Gunnell, 2001b; Chaubey *et al.*, 2002; Rao *et al.*, 2002), seismic profiles (Singh *et al.*, 1999; Chaubey *et al.*, 2002) and isopach maps (Rao & Srivastava, 1984). Total sediment thickness is based on the isopach maps of Rao and Srivastava (1984) and Rao *et al*. (2002).

A regional seismic survey by Rao and Srivastava (1984) derived three major Cenozoic sedimentary sequences in the Konkan-Kerala basin (fig. 5): a lower succession, sequence II, with sediments of Palaeogene age ranging in thickness from 200 ms to 1200 ms TWT; a middle succession, sequence III, of Miocene sediments ranging in thickness from 200 ms to 1200 ms TWT; and an upper succession, sequence IV, of post-Miocene sediments ranging in thickness from 20 ms to 120 ms TWT. By contrast, Chaubey *et al*. (2002) identified six Cenozoic sequences (H1 to H6) on the basis of a multi-channel seismic reflection profile across the northern part of the Konkan Kerala Basin (Figs 2 and 5). We have combined the sequences of Chaubey *et al*. (2002) with the three broad sedimentary sequences of Rao and Srivastava (1984). The boundary between Chaubey *et al*. (2002) sequences H2 and H3 has an inferred age of Late Oligocene (Chaubey *et al*. (2002) Table 1, p.306) and thus correlates well with Rao and Srivastava (1984) boundary between sequences.II and III. Similarly, the boundary between Chaubey *et al*. (2002) sequences H5 and H6 is Late Pleistocene and correlates well with the boundary between Rao and Srivastava (1984) sequences III and IV. The relationships between the chronologies of Chaubey *et al*. (2002) and Rao and Srivastava (1984) are summarised in Table 1. Our revised chronostratigraphy refines the depositional period for Rao and Srivastava's (1984) sequences II, III and IV.

Importantly, it has been possible to further sub-divide the three broad sequences based on a detailed analysis of the stratigraphy from ten litho-logs collected throughout the Konkan-Kerala basin, and an additional stratigraphic column from onshore Kerala. These five sub-divisions (IV, IIIa, IIIb, IIa and IIb) and their equivalent ages are displayed in Figure 4, and have been used for the sediment volume calculations. Figure 6 gives a simplified cross section through the northern part of the basin based on the seismic profile of Chaubey *et al*. (2002) together with the topographic profile onshore of this section.

Sediment volumes were calculated by digitizing the sediment isopach maps of Rao and Srivastava (1984) and importing them into a GIS. Volume calculations for sequences II, III, and IV were then computed in the GIS with the assumption that 1 s two-way travel time is equivalent to 1 km thickness of sediment (e.g., Gunnell & Fleitout, 1998). The sediment thicknesses for each of the three broad sequences in the study area are shown in figure 5. Stratigraphic correlations between the boreholes were used to subdivide sequences II and III into IIa, IIb, IIIa and IIIb respectively (fig. 4). The ratios of sequence IIa:IIb and IIIa:IIIb were then used to calculate the proportion of sediment (both clastic and non-clastic) for each of the sub-divisions. Using lithologies recorded in the eleven boreholes in the study area, percentages of clastic (terrigenous) and non-clastic sediments (biogenic and marine limestones) were obtained for each of the five sequences (IV, IIIa, IIIb, IIa, IIb). The non-clastic component of each of the sequences was then removed from the individual volumes, thereby to acquire the compacted clastic components.

Finally, to obtain true sediment volumes the clastic volumes were decompacted to allow for the effects of sediment loading with depth. For this we assumed an exponential relationship between depth and sediment porosity following the procedure of Allen & Allen (2005) and using the following equation:

$$y_2' - y_1' = y_2 - y_1 - \tfrac{\phi_0}{c}\left[\exp(-cy_1) - \exp(-cy_2)\right] + \tfrac{\phi_0}{c}\left[\exp(-cy_1') - \exp(-cy_2')\right] \qquad [1]$$

where y'_2 and y_2 are the decompacted and compacted depths respectively to the base of the layer, y'_1 and y_1 are the decompacted and compacted depth respectively to the top of the layer ($y'_1 = 0$ for decompaction to sea level). The term Φ_0 is a constant for the initial porosity prior to compaction (0.56 for shaley sandstone, the most abundant terrigenous sediment in the basin (Rao & Srivastava, 1984; Chaubey *et al.*, 2002). The porosity coefficient (c) is a constant which describes the gradient of the porosity-depth curve (0.39 for shaley sandstone). Equation [1] is equivalent to 'sliding' a given sedimentary layer up the porosity-depth curve. Average depths for the top and base of each of the five sedimentary layers were used and their percentage increases in thickness were applied to their decompacted volumes. For example, the average depths to the base and top of sequence IIa are 2900m and 1000m respectively, giving an average compacted thickness of 1900m. If sequence IIa is decompacted, the thickness increases to 2200 m or by 15%. This 15% increase is then applied to the compacted volume for sequence IIa to give a true decompacted volume.

There are two potential further sources of sediment which have not been accounted for in these mass balance calculations, namely, dissolved non-clastic material derived from chemical weathering, and clastic sediment sourced from the conjugate margins of Madagascar and the Seychelles. The non-clastic component of sediment is not included in the mass balance calculations, yet a proportion of carbonate sediments must be derived from the dissolution, chelation and weathering of Ca-bearing minerals onshore. Tropical weathering conditions are likely to have been significant in Western India;

however, dissolved calcium is difficult to quantify and there are only approximate present day estimates available for Western India (Dessert *et al.*, 2001; Das *et al.*, 2005; Prasad & Ramanatran, 2005). Sediment derived from the conjugate margins (Seychelles or Madagascar) likewise could have contributed sediment to the Konkan-Kerala basin. Madagascar rifted from Greater India at 88Ma (Storey, 1995), with pre-Cretaceous sediments being restricted to the deeper central grabens within the basin. These early sedimentary successions have not been included in the sediment volume calculations. Similarly, the development of the Carlsberg ridge separated India from the Seychelles at 65 Ma, and accordingly, there is little sediment contribution from the low-lying Seychelles microcontinent (Plummer & Belle, 1995). Where elevations on the microcontinent are significant, sediments are carbonate-dominated and not extensive

Sediment mass balance

A simple mass balance study is possible for the Konkan-Kerala basin because the clastic sediments are essentially derived from the adjacent onshore portion of the margin (Rao & Rao, 1995). The source of sediment onshore is defined as the area seaward (to the west) of the regional watershed (Figure 2). Easterly- and westerly-flowing river basins were extracted from the GTOPO30 DEM in order to define the regional watershed between these catchments, which forms the eastern limit of the study area. The northern limit of the sediment source area is onshore of the northern margin of the Konkan-Kerala basin east of the Vengurla arch basement high, and the southern limit is the tip of the Indian peninsula (Figure 2). The offshore sediment volume is a combination of the volume of prism eroded from the coastal plain (use to test the different conceptual models) and the additional volume eroded between the escarpment lip and the regional watershed (fig 7).

The DEM was used to calculate the onshore area and volume of crust that might have existed prior to denudation of the coastal plain. Most critically, the volume of eroded crust depends on the geometry of the upper surface of the eroded prism, which is itself controlled by both the geometry of the syn-rift palaeosurface and the flexural strength of the lithosphere. Flexurally strong lithosphere will resist the denudational isostasy resulting from denudation of the prism, and so the prism of material removed will either be rectangular in its cross-section (i.e. where the prism has a horizontal upper surface corresponding to a syn-rift palaeosurface extending horizontally seawards from the crest of the escarpment) or the prism will be wedge-shaped in form, thinning towards the coast (Fig. 7a). A wedge-shaped prism is analogous to a downwarped margin geometry where syn-rift downwarping occurs, thereafter the lithosphere remains flexurally rigid (Ollier, 1982; Ollier & Pain, 1997). By contrast a flexurally weaker lithosphere will rebound through denudational unloading, thereby increasing the volume of material that is eroded and subsequently transported offshore (Gunnell, 1998). The geometry of a crustal prism depends on the pre-existing palaeo-elevation of the rift shoulder and/or flexural rebound, will be an inverted wedge thickening towards the coast, analogous to the elevated rift flank model (Fig. 7b). Amounts of lithospheric rebound will vary with lithospheric flexural properties, generating different volumes of missing crustal prisms; this matter is explored more fully below.

For the purposes of this work, the eroded volumes were calculated corresponding to (i) a seaward tapering wedge-shaped geometry (Ollier & Pain's (1997) downwarped rift flank), and (ii) an inverted wedge-shaped geometry (elevated rift flank) (fig. 7). The small volume of eroded material between the escarpment lip and the regional watershed was then added to the eroded volume of each crustal prism (fig. 7), constrained using palaeosurface reconstructions from the Deccan volcanic province (Widdowson, 1997) and from the northern Dharwar Craton (Gunnell, 1998). Finally, the chemical weathering contribution has been corrected for by removing 20% (Dessert *et al.*, 2001; Das *et* *al.*, 2005; Prasad & Ramanatran, 2005) from the total eroded volume. Recompacting the decompacted volume of offshore clastic sediment to equivalent crystalline basement rock densities allows a comparison between the offshore sediment volume and onshore denuded material (for different crustal prisms), completing the mass balance. A density of 1200 kg m^{-3} (average for shaley sandstone) was adopted for the sediments and a density of 2700 kg m^{-3} for crystalline rocks (Rust & Summerfield, 1990).

Flexural response of the lithosphere to sedimentation and denudation

The lithosphere compensates for large stresses either locally by Airy isostasy, or regionally by the mechanism of flexural isostasy (Watts, 2001). Offshore sediment loading will load the underlying lithosphere and cause flexural subsidence: if there has been no additional tectonic or thermal subsidence, then the depth to the sediment-basement interface is the result of flexural compensation only (Allen & Allen, 2005). Similarly, the onshore lithosphere responds to denudational unloading by upwards flexural deflection: If there has been no additional tectonic rock uplift or if the pre-rift surface was elevated (and has since been denuded), then the amount of eroded material is a function of the rate of denudation and the flexural response of the lithosphere only.

Regionally-compensated topographic loads that deform the lithosphere are commonly modelled as a loaded, thin, elastic plate overlying a fluid substratum (Hetenyi, 1946; Watts, 2001; Turcotte & Schubert, 2002). Accordingly, the flexural response of the Western Indian margin has previously been modelled as a continuous elastic plate analogous to an infinite beam, or as a broken plate analogous to a semi-infinite beam with one free end (Gunnell & Fleitout, 1998, 2000). The broken plate model simulates a break or fault that effectively de-couples the onshore and offshore portions of the margin. The much-debated West Coast Fault putatively located offshore could represent such a de-coupling zone (Chandrasekharam, 1985; Balakrishnan, 2001). We here calculate the flexural deflection of the lithosphere to sediment loading offshore for the Konka-Kerala basin and denudational unloading onshore for Western India. The lithospheric flexure resulting from a load of a continuous plate [eq. 2] and broken plate [eq. 3] can be defined following Pazzaglia & Gardner (1994) and Watts (2001) as:

$$W_b(x) = W_0 e^{\frac{-x}{a}} (\frac{\cos x}{\alpha} + \frac{\sin x}{\alpha}) \qquad [2]$$

$$W_b(x) = W_o e^{\frac{-x}{/\alpha}} \frac{\cos x}{\alpha} \qquad [3]$$

where $W_b\,(x)$ is the deflection at distance x from is the maximum deflection at the point of loading and is defined as:

$$W_0 = \frac{q\alpha^3}{8D} \qquad [4]$$

where

$$D = \frac{ET_e^3}{12(1-\nu^2)} \qquad [5]$$

D, the flexural rigidity is the relationship between plate elasticity (E), Poisson's ratio (v) and the effective elastic thickness (T_e). The effective elastic thickness varies depending on the rheology, age and structure of the lithosphere. Estimates of T_e for continental lithosphere range between 5km and 70km (Watts, A. B., 2001). The flexural parameter (α) and flexure (q) are defined by the following relationships (Pazzaglia, F. J. & Gardner, T. W., 1994):

$$\alpha^4 = \frac{4D}{\rho_m g} \qquad [6]$$

$$q = \rho_s g \Delta xy \qquad [7]$$

where ρ_s and ρ_m are sediment and mantle densities, g is the acceleration due to gravity (i.e., 9.8 ms^{-2}). The sediment cross-section that is loading (or unloading) the lithosphere at a particular point is defined as Δxy (fig. 8). Distributed loads of various sizes result in contrasting flexural responses such that a narrow load flexes the lithosphere differently to a wide load. Determining the geometry of the cross sectional area is critical in order to model the flexural response of sediment loading and denudational unloading accurately. The effective elastic thickness (T_e) is a theoretical thickness that is attributed to a thermal layer within oceanic lithosphere (Watts, 1978; Watts & Burov, 2003) but its physical meaning within continental lithosphere is unclear (Burov & Diament, 1995, 1996; Stuwe, 2001). The effective elastic thickness is, nonetheless, a useful variable for altering the flexural properties of the lithosphere. Modifying T_e provides different magnitudes and geometries of deflection such that low T_e values generate large amounts of flexure over short distances and large T_e values generate lower amounts of flexure but over greater distances. The parameter values for modelling flexure of the lithosphere are listed in Table 2.

The modelled lithosphere was split into eight cells, five 100 km wide cells representing the lithosphere offshore and three the lithosphere onshore (one 50 km wide cell seaward of the escarpment and two 100 km wide cells landward of the escarpment). The present day coast was taken as the boundary between the loaded offshore section of lithosphere and the unloaded onshore section of the lithosphere. Although the position of the coastline is largely a function of Holocene eustatic sea level rise it nonetheless marks the boundary between onshore denudation and offshore deposition. It is recognised that the position of the coast will have altered throughout the geological history of the Western Indian margin; however, there are no adequate constraints on coastal palaeoposition so the simplifying assumption is made that the coastline has, on average, effectively remained constant.

The flexural responses for each of the cells in the cross-section (including the flexural effects on neighbouring cells) were modelled for both continuous and discontinuous plates. The Δxy values for each of the five cells loading the lithosphere offshore were obtained by taking the average decompacted sediment thicknesses along strike from their position offshore using the sediment isopach maps of Rao & Srivastava (1984). The Δxy value for the cell seaward of the escarpment was obtained using the re-compacted total clastic sediment thickness from the mass balance estimates, and the Δxy values for the two cells landward of the escarpment were obtained by assuming that 500 m of lithosphere has been denuded from the interior plateau since the onset of rifting. This is a reasonable value because removal of ca. 500m Deccan lavas inland of the escarpment north of the study area has been estimated (Widdowson, 1997). The flexural effects from each loaded cell and the flexural effects from loaded neighbouring cells were then summed to provide the total deflection at a particular point along the modelled plate (fig. 9).Published constraints for the effective elastic thickness of the Indian sub-continent are rare and are summarised in Table 4.

As a consequence of the large range of published T_e estimates for Western Indian we have used T_e values ranging from 10 km to 70 km. The oceanic/continental crust transition is thought to occur west of the Chagos-Laccadive ridge (Kolla & Coumes, 1990), therefore the lithosphere beneath the Konkan-Kerala basin has similar rheological properties to the adjacent onshore lithosphere and their flexural properties (including T_e) should also be similar. The flexural isostatic response of the lithosphere is modelled to determine if the amount of subsidence offshore and the amount of denudation onshore can be explained by flexural isostasy alone or if additional mechanisms are required.

RESULTS

Sediment volumes and fluxes

The Konkan-Kerala basin contains an estimated total sediment volume (clastic and carbonate) of 464,000km^3; the total clastic volumes and decompacted clastic volumes for each sequence are given in Table 5. The decompacted sediment volume and the depositional duration for each of the five sequences (the latter constrained by the borehole stratigraphy) allow clastic sediment volume accumulation rates to be calculated. Estimated onshore volumes of rock are also included in Table 5 as recompacted sediment volumes equivalent to crystalline basement. The final column of Table 5 gives the onshore denudation rates equivalent to the volumes of sediment in sequences IIb, IIa and IIIb. The depositional duration of sequence IV is only 0.08 Ma, which implies unrealistically high denudation rates, and so the denudation rates of sequences IIIa and IV have been combined.

Sequences IIb, IIIa and IV have much greater proportions of clastic sediment compared to sequences IIa and IIIb which are carbonate-dominated. Clastic sediment accumulation rates mirror this, with peak accumulation rates in the Palaeocene and Pliocene, separated by an intervening period of low clastic accumulation rates throughout the Eocene, Oligocene and Miocene (Fig. 10).

The total equivalent rock volume calculated from the combined volumes of re-compacted clastic sediment is estimated to be 109,000 km^3. The onshore source area for these sediments comprises of 6 $x10^4$ km^2 for the area between the escarpment and the coast, and 2.3 $x10^4$ km^2 for the area between the escarpment and the regional watershed (total of 8.3 $x10^4$ km^2). The total volume of denuded lithosphere (including the contribution landward of the escarpment lip) for a seaward tapering wedge-shaped prism (Ollier & Pain's (1997) downwarp geometry) is 38,000 km^3. Accordingly, denudation of a downwarped wedge-shaped prism accounts for ~ 30% of the offshore sediments . By contrast, an inverted wedge-shaped prism with 3 km of rebound at the coast (decreasing to 1.2 km at the escarpment) has a volume of 110,000 km^3, an amount more obviously consistent with the volume of sediment calculated as being present offshore.

Flexural isostasy modelling

We here model the flexural isostatic response of the lithosphere for a continuous plate (Table 6) and broken plate (Table 7) with a range of effective elastic thicknesses. Results are summarised in Figure 11. In general, as the lithosphere becomes progressively more rigid (higher effective elastic thicknesses), the vertical amplitude of flexural deflection decreases. The maximum vertical amplitude of flexural deflection (both offshore and onshore) tends to be greater for a continuous plate configuration as opposed to a broken plate configuration because in the former there is no de-coupling between the offshore and onshore areas. With a continuous plate, the flexural effects from cells offshore are transmitted as a peripheral foreland bulge onshore and vice versa. This interaction is most significant for high values of effective elastic thickness (more rigid lithosphere) where the vertical amplitude of flexural deflection is smaller but is transmitted over larger distances.

Flexural modelling was undertaken to ascertain whether the flexural response of the lithosphere could account for the magnitude and position of maximum subsidence offshore and denudation onshore. The maximum depth to the sediment-basement interface (2.5 km; measured directly from the cross section) is greatest in the centre of the basin, at an average distance from coast of 150km. The modelled flexural deflection as a consequence of sediment loading, even for a lithosphere with a T_e value of 10 km, cannot account for the current depth to the sediment-basement interface in the centre of the basin. Therefore, additional tectonic or thermal subsidence must be invoked to explain the observed configuration. The measured distance from the coast to the centre of the basin corresponds well to the modelled distance from the coast to the point of maximum flexure (i.e. analogous to the flexural wavelength).

Mass balance analysis indicates that, for an inverted denuded crustal prisms (analogous to the elevated rift flank model), 3 km of downwearing at the coast decreasing to 1.2 km downwearing at the escarpment is sufficient to account for the volume of sediment present offshore. Modelling of lithosphere with a T_e value of 10 km predicts sufficient onshore flexural deflection to account for the magnitude of downwearing at the escarpment (i.e. 1.2 km) and does not require any additional mechanisms to generate denudation. However, even a low $\mathrm{T_e}$ of 10 km is insufficient to account for the 3 km of denudation required at the coast for an inverted missing wedge of crustal material. A lithosphere with T_e values between 10 km and 30km also generates maximum flexure on the coastal plain, whereas flexurally stronger lithosphere (T_e = 50 - 70 km) corresponds to maximum values of flexure inland of the escarpment on the interior plateau. The geomorphology and geology suggest that there has only been ca. 500 m of downwearing inland of the escarpment (Widdowson, 1997); therefore, if flexural isostasy is the sole mechanism for generating denudation then a flexurally weak lithosphere is required.

DISCUSSION

There are two maxima in offshore sedimentation rates, pointing to two maxima in onshore denudation. The first maximum in sedimentation rates, beginning in the Palaeocene (Sequence IIb), is likely the result of rift-flank denudation and escarpment formation in response to breakup between Western India and the Seychelles at ca. 65 Ma. The second maximum in sedimentation rates occurred after the Late Miocene (i.e., Sequences IIIa and IV). This younger phase cannot be readily related to the initial surface uplift in response to rifting, and, if real, the mechanisms responsible remain unclear.

Gunnell *et al*. (2003) conducted an extensive apatite fission track study to resolve the thermal history of the Western Indian margin. Modelled thermal histories indicate that a sharp increase in denudation occurred at the start of the Cenozoic, which is contemporaneous with the increase in sedimentation recorded in the offshore sedimentary record (Fig. 12). However, these thermochronometric data fail to identify the observed post-Miocene increase in sedimentation. The average amount of downwearing predicted from the mass balance study across the coastal plain throughout the Cenozoic for an elevated rift flank is 3 km at the coast decreasing to 1.2 km at the escarpment (Fig. 6b). Magnitudes of denudation between 1 and 2 km do not reset AFT ages and approach the sensitivity limits of the AFTT system (Braun & van der Beek, 2004). The absence of the post-Miocene increase in sedimentation (and hence denudationally induced cooling) within the AFTT record may thus be a consequence of the limits of the technique.

The downwarped rift flank model proposed by King (1967), and Ollier & Pain (1997) incorporates a flexurally rigid lithosphere and as such only envisages small magnitudes of denudation, which is incompatible with the volume of clastic sediment present offshore. The downwarp model has been subsequently modified for the Deccan Volcanic Province not only to account for the monoclinal structure of this segment of the margin (Auden, 1949) but also to include ongoing post-rift flexural uplift (Widdowson & Cox, 1996; Widdowson, 1997). The question remains whether this modified downwarp model also applies to the segment of the margin south of the Deccan Volcanic Province. The volume of clastic sediment within our study area can only be accounted for if there is denudational isostasy, which in figure 6b, is modelled as a component of the elevated rift flank model. However, sediment mass balance alone does not have the spatial resolution to differentiate between the elevated rift flank model and the modified downwarp model. The volume of clastic sediment could equally be explained by a denuded prism ~ 2 km thick similar to the modified downwarp model illustrated in Widdowson's (1997) figure 12. Apatite fission track thermochronometry is capable of resolving the spatial differences in denudation between the elevated rift flank model (greatest magnitude of denudation at the coast) and the modified downwarp model (greatest denudation at the escarpment). The AFTT data suggest between 3 and 4 km of denudation close to the coast, but AFTT data from further inland on the coastal plain suggest more modest amounts of unroofing of between 1.5km and 2.5km (Gunnell *et al.*, 2003). Data from apatite fission track thermochronometry along the west coast of India are thus more consistent with the elevated rift flank model.

If our study area has developed into an elevated rift flank, this poses additional challenges in generating a model for the evolution of Western India by implicating a tectonically and geomorphically segmented margin. Further work must be undertaken to improve our understanding of the spatial pattern of denudation for the onshore hinterland. It is unclear if the magnitude of cooling at the coast predicted from AFTT is a consequence of denudationally induced rock uplift (supporting the elevated rift flank model) or an increase in the palaeogeothermal gradient due to rift related lithospheric thinning and/or the passage of the Reunion plume.

Flexural isostasy is an important requirement for elevated rift flank model and modelling results suggest that a flexural response to sediment loading offshore and denudation onshore can play an important role. Flexural isostasy alone cannot produce a significant amount subsidence offshore, and is thus unlikely to be the sole mechanism for such subsidence. However, flexural isostasy can generate sufficient rock uplift onshore close to the escarpment provided that the lithosphere has a T_e of 10 km. The magnitude of denudation at the coast for the elevated rift flank model is constrained using AFTT, but the 3 km of unroofing necessary to produce the clastic sediment offshore cannot be adequately account for by a flexural response to denudational unloading. The 3 km of unroofing at the coast could be a combination of flexural uplift and a pre-existing elevated rift flank (i.e. additional palaeoelvation) present at the onset of rifting.

CONCLUSIONS

Isopach maps and lithologs have made it possible to divide the Konkan-Kerala basin into five sub-sequences of post rift sedimentation since the Late Cretaceous. Sediment volumes indicate two major pulses in clastic deposition: one immediately after rifting of the Seychelles microcontinent from India (sequence IIb) and a second in the Pliocene (sequences IIIa and IV). These two phases of enhanced sedimentation are separated by an intervening period of quiescence dominated by carbonate deposition (sequences IIa and IIIb).

Clastic deposition rates immediately after rifting, represented by sequence IIb, are high (11,522 km^3 Myr^{-1}). Rates decrease to a low of 183 km^3 Myr^{-1} during the Palaeogene, represented by sequences IIa and IIb. A second rise in deposition rates began in the Pliocene (sequence IIIa) peaking at 462 500 km^3 Myr^{-1} in the Pleistocene (sequence IV). These values equate to 0.56 km of downwearing during the post rift phase, 0.66 km during the second, later higher phase and an intervening period of very low denudation of only 0.08km onshore.

Sediment mass balance confirms that denudation of an Ollier and Pain (1997) downwarped rift shoulder does not yield sufficient sediment to account for the clastic accumulations in the Konkan-Kerala basin. It seems unlikely that additional sources of sediment such as from the conjugate margin or longshore transportation can generate all of the ‘excess’ sediment that is not accounted for by denudation of the triangular wedge of a downwarped margin. Rather, denudation of either a modified downwarped rift flank (Widdowson, 1997) or an elevated rift flank both accompanied by lithospheric flexure in response to denudational unloading onshore offers a better explanation for the large volumes of sediment preserved offshore. Despite the implications for a tectonically divided margin, this study prefers the elevated rift flank model on the basis of denudational constraints provided from AFTT.

This study highlights the importance of offshore sedimentation records in understanding passive margin evolution. Offshore basins provide an almost continuous record of the depositional (and hence erosional) history where stratigraphic markers on the adjacent onshore margin are scant. The application of such studies combined with low temperature thermochronology onshore will undoubtedly advance our knowledge of the development of passive margins.

(B) Acknowledgements:

DC is funded by an Ocean Margins PhD studentship funded by the Natural Environment Research Council (NER/S/R/2003/12016). We thank the Commonwealth Scholarship Commission in the United Kingdom and the British Council for an Academic Fellowship for CGN to visit UK. We thank A. T. Codilean for assisting with the computations and O. Fernandez at Dhempe Colege, Goa. Yanni

Gunnell and Frank Pazzaglia provided very helpful reviews that improved an earlier version of this manuscript.

(B) REFERENCES

ALLEN, P.A. & ALLEN, J.R. (2005) *Basin Analysis*. Blackwell Science (UK).

AUDEN, J.B. (1949) Dykes in Western India - a Discussion of Their Relationship with the Deccan Traps. *Transactions of the National Institute of Science, India*, **3,** 123-159.

BALAKRISHNAN, T.S. (2001) Tectonics of Western India Inferred from Gravity Patterns and Geophysical Exploration. In: *Sahyadri, the Great Escarpment of the Indian Subcontinent. Patterns of Landscape Development in the Western Ghats* (Ed. by Y. Gunnell & B. P. Radhakrishna), 271-278. Geological Society of India, Bangalore.

BECKINSALE, R.D., DRURY, S.A. & HOLT, R.W. (1980) 3,360-Myr Old Gneisses from the South Indian Craton. *Nature*, **283,** 469-470.

BESSE, J. & COURTILLOT, V. (1988) Paleogeographic Maps of the Continents Bordering the Indian Ocean since the Early Jurassic. *Journal of Geophysical Research-Solid Earth and Planets*, **93,** 11791-11808.

BESSE, J. & COURTILLOT, V. (1991) Revised and Synthetic Apparent Polar Wander Paths of the African, Eurasian, North American and Indian Plates, and True Polar Wander since 200 Ma. *Journal of Geophysical Research-Solid Earth and Planets*, **96,** 4029-4050.

BRAUN, J. & VAN DER BEEK, P. (2004) Evolution of Passive Margin Escarpments: What Can We Learn from Low-Temperature Thermochronology? *Journal Of Geophysical Research-Earth Surface*, **109**.

BROWN, R.W., RUST, D.J., SUMMERFIELD, M.A., GLEADOW, A.J.W. & DE WIT, M.C.J. (1990) An Early Cretaceous Phase of Accelerated Erosion on the South-Western Margin of Africa: Evidence from Apatite Fission Track Analysis and the Offshore Sedimentary Record. *Nuclear Tracks and Radiation Measurement*, **17,** 339-350.

BUROV, E. & DIAMENT, M. (1996) Isostasy, Equivalent Elastic Thickness, and Inelastic Rheology of Continents and Oceans. *Geology*, **24,** 419-422.

BUROV, E.B. & DIAMENT, M. (1995) The Effective Elastic Thickness (T-E) of Continental Lithosphere - What Does It Really Mean. *Journal Of Geophysical Research-Solid Earth*, **100,** 3905-3927.

CHAND, S. & SUBRAHMANYAM, C. (2003) Rifting between India and Madagascar - Mechanism and Isostasy. *Earth And Planetary Science Letters*, **210,** 317-332.

CHANDRASEKHARAM, D. (1985) Structure and Evolution of the Western Continental Margin of India Deduced from Gravity, Seismic, Geomagnetic and Geochronological Studies. *Physics of The Earth and Planetary Interiors*, **41,** 186-198.

CHAUBEY, A.K., RAO, D.G., SRINIVAS, K., RAMPRASAD, T., RAMANA, M.V. & SUBRAHMANYAM, V. (2002) Analyses of Multichannel Seismic Reflection, Gravity and Magnetic Data Along a Regional Profile across the Central-Western Continental Margin of India. *Marine Geology*, **182,** 303-323.

CLIFT, P.D., SHIMIZU, N., LAYNE, G.D., BLUSZTAJN, J.S., GAEDICKE, C., SCHLUTER, H.U., CLARK, M.K. & AMJAD, S. (2001) Development of the Indus Fan and Its Significance for the Erosional History of the Western Himalaya and Karakoram. *Geological Society Of America Bulletin*, **113,** 1039-1051.

COCKBURN, H.A.P., BROWN, R.W., SUMMERFIELD, M.A. & SEIDL, M.A. (2000) Quantifying Passive Margin Denudation and Landscape Development Using a Combined Fission-Track Thermochronology and Cosmogenic Isotope Analysis Approach. *Earth and Planetary Science Letters*, **179,** 429-435.

COURTILLOT, V., BESSE, J., VANDAMME, D., MONTIGNY, R., JAEGER, J.J. & CAPPETTA, H. (1986) Deccan Flood Basalts at the Cretaceous Tertiary Boundary. *Earth and Planetary Science Letters*, **80,** 361-374.

COX, K.G. (1980) A Model for Flood Basalt Vulcanism. *Journal of Petrology*, **21,** 629-650.

DAS, A., KRISHNASWAMI, S., SARIN, M.M. & PANDE, K. (2005) Chemical Weathering in the Krishna Basin and Western Ghats of the Deccan Traps, India: Rates of Basalt Weathering and Their Controls. *Geochimica et Cosmochimica Acta*, **69,** 2067-2084.

DESSERT, C., DUPRE, B., FRANCOIS, L.M., SCHOTT, J., GAILLARDET, J., CHAKRAPANI, G. & BAJPAI, S. (2001) Erosion of Deccan Traps Determined by River Geochemistry: Impact on the Global Climate and the Sr-87/Sr-86 Ratio of Seawater. *Earth And Planetary Science Letters*, **188,** 459-474.

DRURY, S.A., HOLT, R.W., VANCLASTEREN, P.C. & BECKINSALE, R.D. (1983) Sm-Nd and Rb-Sr Ages for Archean Rocks in Western Karnataka, South-India. *Journal Of The Geological Society Of India*, **24,** 454-459.

GHOSH, B.N. & ZUTSHI, P.L. (1989) Indian West Coast Shelf Break Tectonic Features. *Geological Survey of India Special Publication*, **24,** 309-318.

GILCHRIST, A.R. & SUMMERFIELD, M.A. (1990) Differential Denudation and Flexural Isostasy in Formation of Rifted Margin Upwarps. *Nature*, **346,** 739-742.

GILCHRIST, A.R. & SUMMERFIELD, M.A. (1994) Tectonic Models of Passive Margin Evolution and Their Implications for Theories of Long-Term Landscape Development. In: *Process Modles and Theoretical Geomorphology* (Ed. by M. J. Kirkby), 55-84. John Wiley & Son Ltd., Chichester.

GILCHRIST, A.R., SUMMERFIELD, M.A. & COCKBURN, H.A.P. (1994) Landscape Dissection, Isostatic Uplift, and the Morphologic Development of Orogens. *Geology*, **22,** 963-966.

GOMBOS, A.M., POWELL, W.G. & NORTON, I.O. (1995) The Tectonic Evolution of Western India and Its Impact on Hydrocarbon Occurrences - an Overview. *Sedimentary Geology*, **96,** 119-129.

GOWD, T.N., RAO, S.V.S. & GAUR, V.K. (1992) Tectonic Stress-Field in the Indian Subcontinent. *Journal of Geophysical Research-Solid Earth*, **97,** 11879-11888.

GUNNELL, Y. (1997) Relief and Climate in South Asia: The Influence of the Western Ghats on the Current Climate Pattern of Peninsular India. *International Journal of Climatology*, **17,** 1169-1182.

GUNNELL, Y. (1998) The Interaction between Geological Structure and Global Tectonics in Multistoreyed Landscape Development: A Denudation Chronology of the South Indian Shield. *Basin Research*, **10,** 281-310.

GUNNELL, Y. & FLEITOUT, L. (1998) Shoulder Uplift of the Western Ghats Passive Margin, India: A Denudational Model. *Earth Surface Processes and Landforms*, **23,** 391-404.

GUNNELL, Y. & FLEITOUT, L. (2000) Morphotectonic Evolution of the Western Ghats, India. In: *Geomorphology and Global Tectonics* (Ed. by M. A. Summerfield), 321-338. John Wiley & Sons Ltd., Chichester.

GUNNELL, Y. (2001a) Dynamics and Kinematics of Rifting and Uplift at the Western Continental Margin of India: Insights from Geophysical and Numerical Models. *Geological Society of India, Bangalore*, **47,** 475-496.

GUNNELL, Y. (2001b) Fluvial Routing Systems and the Signatures of Onshore Denudation in the Offshore Sedimentary Record of Western India. *Geological Society Of India*, **47,** 279-293.

GUNNELL, Y. & RADHAKRISHNA, B.P. (2001) *Sahyadri, the Great Escarpment of the Indian Subcontinent. Patterns of Landscape Development in the Western Ghats*. Geological Society of India, Bangalore.
GUNNELL, Y., GALLAGHER, K., CARTER, A., WIDDOWSON, M. & HURFORD, A.J. (2003) Denudation History of the Continental Margin of Western Peninsular India since the Early Mesozoic - Reconciling Apatite Fission-Track Data with Geomorphology. *Earth and Planetary Science Letters*, **215,** 187-201.
HETENYI, M. (1946) *Beams on Elastic Foundation*. The University of Michigan Press.
HOOPER, P.R. (1990) The Timing of Crustal Extension and the Eruption of Continental Flood Basalts. *Nature*, **345,** 246-249.
JERRAM, D.A. & WIDDOWSON, M. (2005) The Anatomy of Continental Flood Basalt Provinces: Geological Constraints on the Processes and Products of Flood Volcanism. *Lithos*, **79,** 385-405.
JOSEPH, S. & NAMBIAR, C.G. (1996) Alkaline Nature and Taphrogenetic Affinity of Felsic Volcanic Rocks of St Mary Islands, Off Mangalore Coast. *Current Science*, **70,** 858-860.
KALASWAD, S., RODEN, M.K., MILLER, D.S. & MORISAWA, M. (1993) Evolution of the Continental-Margin of Western India - New Evidence from Apatite Fission-Track Dating. *Journal Of Geology*, **101,** 667-673.
KEAREY, P. & VINE, F.J. (1996) *Global Tectonics*. Blackwell Science, Oxford.
KESSARKAR, P.M., RAO, V.P., AHMAD, S.M. & BABU, G.A. (2003) Clay Minerals and Sr-Nd Isotopes of the Sediments Along the Western Margin of India and Their Implication for Sediment Provenance. *Marine Geology*, **202,** 55-69.
KING, L.C. (1955) Pediplanation and Isostasy: An Example from South Africa. *Quarterly Journal of the Geological Society of London*, **111,** 353-359.
KING, L.C. (1967) *The Morphology of the Earth (2nd Edn.)*. Olliver & Boyd, Edinburgh.
KOLLA, V. & COUMES, F. (1990) Extension of Structural and Tectonic Trends from the Indian Subcontinent into the Eastern Arabian Sea. *Marine and Petroleum Geology*, **7,** 188-196.
KOOI, H. & BEAUMONT, C. (1994) Escarpment Evolution on High Elevation Rifted Margins - Insights Derived from a Surface Processes Model That Combines Diffusion, Advection, and Reaction. *Journal of Geophysical Research-Solid Earth*, **99,** 12191-12209.
KRISHNAN, M.S. (1960) *Geology of India and Burma (4th Edn)*. Higginbothams Ltd. Madras.
MATHUR, R.B. & NAIR, K.R. (1993) Exploration of the Bombay Offshore Basin. *Processess of the Second Seminar on Petroleum Basins of India. KDMIPE and ONGC*, **2,** 365-396.
MATMON, A., BIERMAN, P. & ENZEL, Y. (2002) Pattern and Tempo of Great Escarpment Erosion. *Geology*, **30,** 1135-1138.
MCHARGUE, T.R. & WEBB, J.E. (1986) Internal Geometry, Seismic Facies, and Petroleum Potential of Canyons and Inner Fan Channels of the Indus Submarine Fan. *Aapg Bulletin-American Association Of Petroleum Geologists*, **70,** 161-180.
MCKENZIE, D. & SCLATER, J.G. (1971) Evolution of Indian Ocean since Late Cretaceous. *Geophysical Journal of the Royal Astronomical Society*, **24,** 437-&.
MCKENZIE, D. (1978) Some Remarks on Development of Sedimentary Basins. *Earth and Planetary Science Letters*, **40,** 25-32.
MILES, P.R. & ROEST, W.R. (1993) Earliest Sea Floor Spreading Magnetic Anomalies in the North Arabian Sea and the Ocean-Continent Transition. *Geophysical Journal International*, **115,** 1025-1031.

MOLNAR, P. (2004) Late Cenozoic Increase in Accumulation Rates of Terrestrial Sediment: How Might Climate Change Have Affected Erosion Rates? *Annual Review of Earth and Planetary Sciences.*, **32,** 67-89.

NAINI, B.R. & TALWANI, M. (1982) Structural Framework and the Evolutionary History of the Continental Margin of Western India. In: *Studies in Continental Margin Geology* (Ed. by J. S. Watkins & C. L. Drake), **34**, 167-191. Am. Assoc. Pet. Geol. Mem.

NAIR, K.M., PADMALAL, D. & KUMARAN, K.P.N. (2006) Quaternary Geology of South Kerala Sedimentary Basin - an Outline. *Journal Of The Geological Society Of India*, **67,** 165-179.

NAQVI, S.M. & ROGERS, J.J.W. (1987) Precambrian Geology of India. Oxford Monographs on Geology and Geophysics. In: *Oxford Monographs on Geology and Geophysics* (Ed. by, **No. 6**. Oxford University Press, Oxford.

NORTON, I.O. & SCLATER, J.G. (1979) Model for the Evolution of the Indian-Ocean and the Breakup of Gondwanaland. *Journal Of Geophysical Research*, **84,** 6803-6830.

OLLIER, C.D. (1982) Geomorphology and Tectonics of the Dorrigo Plateau, Nsw. *Journal of the Geological Society of Australia*, **29,** 431-435.

OLLIER, C.D. (1985) Morphotectonics of Passive Continental Margins: Introduction. *Zeitschrift Fur Geomorphologie Supplement-band*, **54,** 1-9.

OLLIER, C.D. & PAIN, C.F. (1997) Equating the Basal Unconformity with the Palaeoplain: A Model for Passive Margins. *Geomorphology*, **19,** 1-15.

PANDE, K., SHETH, H.C. & BHUTANI, R. (2001) Ar-40-Ar-39 Age of the St. Mary's Islands Volcanics, Southern India: Record of India-Madagascar Break-up on the Indian Subcontinent. *Earth and Planetary Science Letters*, **193,** 39-46.

PASCOE, E.H. (1964) *A Manual of the Geology of India and Burma*. Government of India Press, Calcutta.

PAZZAGLIA, F.J. & GARDNER, T.W. (1994) Late Cenozoic Flexural Deformation of the Middle U.S. Atlantic Passive Margin. *Journal of Geophysical Research*, **99,** 12143-12157.

PAZZAGLIA, F.J. & BRANDON, M.T. (1996) Macrogeomorphic Evolution of the Post-Triassic Appalachian Mountains Determined by Deconvolution of the Offshore Basin Sedimentary Record. *Basin Research*, **8,** 255-278.

PERSANO, C., STUART, F.M. & BISHOP, P. (2002) Low-T Thermochronology Constraints on the Development of the Australian Great Escarpment. *Geochimica et Cosmochimica Acta*, **66,** A593-A593.

PERSANO, C., STUART, F.M., BISHOP, P. & DEMPSTER, T.J. (2005) Deciphering Continental Breakup in Eastern Australia Using Low-Temperature Thermochronometers. *Journal of Geophysical Research-Solid Earth*, **110**.

PLUMMER, P.S. & BELLE, E.R. (1995) Mesozoic Tectonostratigraphic Evolution of the Seychelles Microcontinent. *Sedimentary Geology*, **96,** 73-91.

PRASAD, M.B.K. & RAMANATRAN, A.L. (2005) Solute Sources and Processes in the Achankovil River Basin, Western Ghats, Southern India. *Hydrological Sciences Journal-Journal Des Sciences Hydrologiques*, **50,** 341-354.

RADHAKRISHNA, B.P. (1967) The Western Ghats of the Indian Peninsula. *Proc. seminars on geomorphological studies in India, Nov, 1965*, 5-13.

RADHAKRISHNA, B.P. (1993) Neogene Uplift and Geomorphic Rejuvenation of the Indian Peninsula. *Current Science*, **64,** 787-792.

RAJU, D.S.N., BHANDARI, A. & RAMESH, P. (1999) Relative Sea Level Fluctuations During Cretaceous and Cenozoic in India. *Bulletin ONGC*, **36,** 185-202.

RAO, P.R. & SRIVASTAVA, D.C. (1984) Regional Seismic Facies Analysis of Western Offshore India. *Bulletin of ONGC*, **21,** 83-96.

RAO, S.V., DASGUPTA, D.K., BHUSHAN, K.S., SRINIVAS, M.S. & GHOSH, D.R. (2002) Sedimentary Processes and Structural Framework of Konkan Basin – Western Offshore, India. *Geological Survey of India Special Publication*, **76,** 43-52.

RAO, V.P. & RAO, B.R. (1995) Provenance and Distribution of Clay Minerals in the Sediments of the Western Continental Shelf and Slope of India. *Continental Shelf Research*, **15,** 1757-1771.

RAO, V.P. & WAGLE, B.G. (1997) Geomorphology and Surficial Geology of the Western Continental Shelf and Slope of India: A Review. *Current Science*, **73,** 330-350.

REEVES, C. & DE WIT, M. (2000) Making Ends Meet in Gondwana: Retracing the Transforms of the Indian Ocean and Reconnecting Continental Shear Zones. *Terra Nova*, **12,** 272-280.

RUST, D.J. & SUMMERFIELD, M.A. (1990) Isopach and Borehole Data as Indicators of Rifted Margin Evolution in Southwestern Africa. *Marine and Petroleum Geology*, **7,** 277-287.

SCHLICH, R. (1982) The Indian-Ocean - Aseismic Ridges, Spreading Centers, and Oceanic Basins. *Ocean Basins and Margins*, **6,** 51-147.

SEIDL, M.A., WEISSEL, J.K. & PRATSON, L.F. (1996) The Kinematics and Pattern of Escarpment Retreat across the Rifted Continental Margin of Se Australia. *Basin Research*, **8,** 301-316.

SINGH, N.K. & LAL, N.K. (1993) Geology and Petroleum Prospects of Konkan-Kerala Basin. In: *Proc. Second Seminar on Petroliferous Basins of India,* (Ed. by S. K. Biswas), **2**, 461-469. Indian petroleum Publishers, Dehra Dun, India.

SINGH, R.P., RAWAT, S. & CHANDRA, K. (1999) Hydrocarbon Potential in Indian Deep Waters. *Exploration Geophysics*, **30,** 83-95.

STEPHEN, J., SINGH, S.B. & YEDEKAR, D.B. (2004) Evidence of Low Lithospheric Strength for the South Indian Shield. *Deep continental studies in India*, **14,** 22-24.

STOREY, B.C. (1995) The Role of Mantle Plumes in Continental Breakup: Case Histories from Gondwanaland. *Nature*, **377,** 301.

STUWE, K. (2001) *Geodynamics of the Lithosphere*. Springer.

SUBRAHMANYAM, V., KRISHNA, K.S., MURTHY, G.P.S., RAO, D.G., RAMANA, M.V. & RAO, M.G. (1994) Structural Interpretation of the Konkan Basin, Southwestern Continental Margin of India, Based on Magnetic and Bathymetric Data. *Geo-Marine Letters*, **14,** 1432-1457.

SUBRAHMANYAM, V., RAO, D.G., RAMANA, M.V., KRISHNA, K.S. & RAO, M.G. (1995) Structure and Tectonics of the Southwestern Continental Margin of India. *Tectonophysics*, **249,** 267-282.

SUMMERFIELD, M.A. (1991) *Global Geomorphology*. John Wiley & Sons, New York.

THAKUR, N.K. & NAGARAJAN, N. (1992) Geotectonic Remobilization of the Lower Crustal Segment of Southern Peninsular India. *Physics of the Earth and Planetary Interiors*, **73,** 153-162.

TIWARI, V.M. & MISHRA, D.C. (1999) Estimation of Effective Elastic Thickness from Gravity and Topography Data under the Deccan Volcanic Province, India. *Earth And Planetary Science Letters*, **171,** 289-299.

TUCKER, G.E. & SLINGERLAND, R.L. (1994) Erosional Dynamics, Flexural Isostasy, and Long-Lived Escarpments - a Numerical Modeling Study. *Journal of Geophysical Research-Solid Earth*, **99,** 12229-12243.

TURCOTTE, D.L. & SCHUBERT, G. (2002) *Geodynamics (2nd Edn)*. Cambridge University Press.

VAIDYANADHAN, R. (1977) Recent Advances in Geomorphic Studies of Peninsular India: A Review. *Indian Journal of Earth Science*, **S. Ray vol.,** 13-35.

WATTS, A.B. (1978) Analysis of Isostasy in the Worlds Oceans.1. Hawaiian-Emperor Seamount Chain. *Journal Of Geophysical Research*, **83,** 5989-6004.

WATTS, A.B. & COX, K.G. (1989) The Deccan Traps: An Interpretation in Terms of Progressive Lithospheric Flexure in Response to a Migrating Load. *Earth And Planetary Science Letters*, **93,** 85-97.

WATTS, A.B. (2001) *Isostasy and Flexure of the Lithosphere*. Cambridge University Press.

WATTS, A.B. & BUROV, E.B. (2003) Lithospheric Strength and Its Relationship to the Elastic and Seismogenic Layer Thickness. *Earth And Planetary Science Letters*, **213,** 113-131.

WIDDOWSON, M. & COX, K.G. (1996) Uplift and Erosional History of the Deccan Traps, India: Evidence from Laterites and Drainage Patterns of the Western Ghats and Konkan Coast. *Earth and Planetary Science Letters*, **137,** 57-69.

WIDDOWSON, M. (1997) Tertiary Palaeosurfaces of the Sw Deccan, Western India: Implications for Passive Margin Uplift. In: *Palaeosurfaces: Recognition, Reconstruction and Paleoenvironmental Interpretation* (Ed. by M. Widdowson), **120**, 221-248. Geological Society of London Special Publication.

WIDDOWSON, M. & GUNNELL, Y. (1999) Lateritization, Geomorphology and Geodynamics of a Passive Continental Margin: The Konkan and Kanara Coastal Lowlands of Western Peninsular India. *Special Publication of the International Association of Sedimentologists*, **27,** 245-274.

WIDDOWSON, M. & MITCHELL, C. (1999) Large-Scale Stratigraphy, Structural and Geomorphological Constraints for Earthquakes in the Southern Deccan Traps, India: The Case for Denudationally-Driven Seismicity. *Memoirs of the Geological Society of India*, **43,** 425-452.

(B) **TABLES AND CAPTIONS**

TWT	**Age**	**Rao & Srivastava (1984)**	**Chaubey *et al.* (2002)**	**Age**
20 – 120	post Miocene	Sequence IV	H6	Late Pleistocene – Recent
200 – 1200	Miocene	Sequence III	H3, H4 & H5	Late Oligocene – Late Pleistocene
200 – 1200	Palaeogene	Sequence II	H1 & H2	Palaeocene – Late Oligocene

Table 1 Comparison between the stratigraphy of the Konkan-Kerala basin defined by Rao & Srivastava (1984) and Chaubey et al. (2002)

V	0.25	E	70 x 10^9 Pa
ρ_s *(offshore)*	1200 kg/m^3	G	9.8 ms^{-2}
ρ_s *(onfshore)*	2700 kg/m^3	Δxy	variable – see results
ρ_m	3300 kg/m^3	T_e	variable – see results

Table 2. Parameters for flexural modelling

	Offshore					**Onshore**		
Cell	**A**	**B**	**C**	**D**	**E**	**F**	**G**	**H**
Dist. from coast (km)	-450	-350	-250	-150	-50	25	125	225
Δxy (km^3)	74	90	109	195	125	100	50	50
ρ_s (kg/m^3)	1200	1200	1200	1200	1200	2700	2700	2700

Table 3 Δxy and ρ_s for individual cells loading and unloading the margin, distance from the coast is the distance to the mid-point of the cell. See text for further explanation.

Author	**T_e values**	**Method**
Watts and Cox (1989)	100 km	Modelling Deccan lava emplacement
Gunnell and Fleitout (1998, 2000)	35 km – 70 km	Finite difference numerical model
Stephen *et al*. (2004)	13 km	Gravity and topographic coherence function
Chand and Subrahmanyam (2003)	8 – 15 km	Gravity and bathymetry spectral analysis
Tiwari and Mishra (1999)	10 km	Gravity and topographic coherence function

Table 4. Published constraints for the effective elastic thickness of the Indian lithosphere

(a) Offshore	Total sediment volume (km^3)	% clastic	Total clastic volume (km^3)	Decompacted clastic volume (km^3)	Depositional duration (Myrs)	Clastic sediment accumulation rates (km^3/Myrs)	Equivalent rock volume (km^3)	Denudation rate (m/Myrs)
IV Late Pleistocene – Recent	40,330	91	37,000	37,000	0.08	462,500	16,300	57.2
IIIa Early Pliocene– Late Pleistocene	94,500	92	87,000	87,500	11.5	7,609	38,900	
IIIb Late Oligocene – Late Miocene	140,000	2	2,800	3,808	16.8	227	1,370	0.9
IIa Eocene – Late Oligocene	89,000	11	9,800	11,400	27.4	416	5,070	2.2
IIb Palaeocene – Eocene	100,000	89	89,000	106,000	9.2	1 11,522	47,100	61.4
						Total equivalent rock volume	**108,740**	

(b) Onshore	Volume of denuded prism between the escarpment and the coast (km^3)	Total volume including material denuded landward of escarpment (km^3)	Total denuded volume corrected for chemical weathering contribution (comparable with offshore)
Ollier & Pain (1997) downwarp model	36,000	47,500	**38,000**
Elevated rift flank model	126,000	137,500	**110,000**

Table 5a Results of sedimentation analysis for sequence IV, IIIa, IIIb, IIa and IIb for the Konkan-Kerala Basin. The denudation rate has been combined for sequence IV and IIIa due to the short depositional duration of Sequence IV

Table 5b Results for the onshore total denuded volume of prisms for a downwarped rift flank and an elevated rift flank (column 2). Column 3 displays the total denuded volume taking into account the contribution of material landward of the escarpment (see fig 7). Column 4 displays the total denuded volume corrected for chemical weathering (~ 20 %) and is directly comparable with the total equivalent rock volume present offshore.

Elastic thickness T_e (km)	Max. deflection offshore (m) (subsidence)	Dist. from coast to max deflection offshore (km)	Max. deflection onshore (m) (uplift)	Dist. from coast to max deflection onshore (km)
10	-1109	150	1350	25
30	-690	150	699	25
50	-598	150	536	125
70	-511	150	532	125

Table 6 Results for a continuous plate

Elastic thickness T_e (km)	Max. deflection offshore (m) (subsidence)	Dist. from coast to max deflection offshore (km)	Max. deflection onshore (m) (uplift)	Dist. from coast to max deflection onshore (km)
10	-1151	150	1510	25
30	-525	150	652	25
50	-425	150	478	25
70	-379	150	402	25

Table 7 Results for a broken plate

(B) FIGURES AND CAPTIONS:

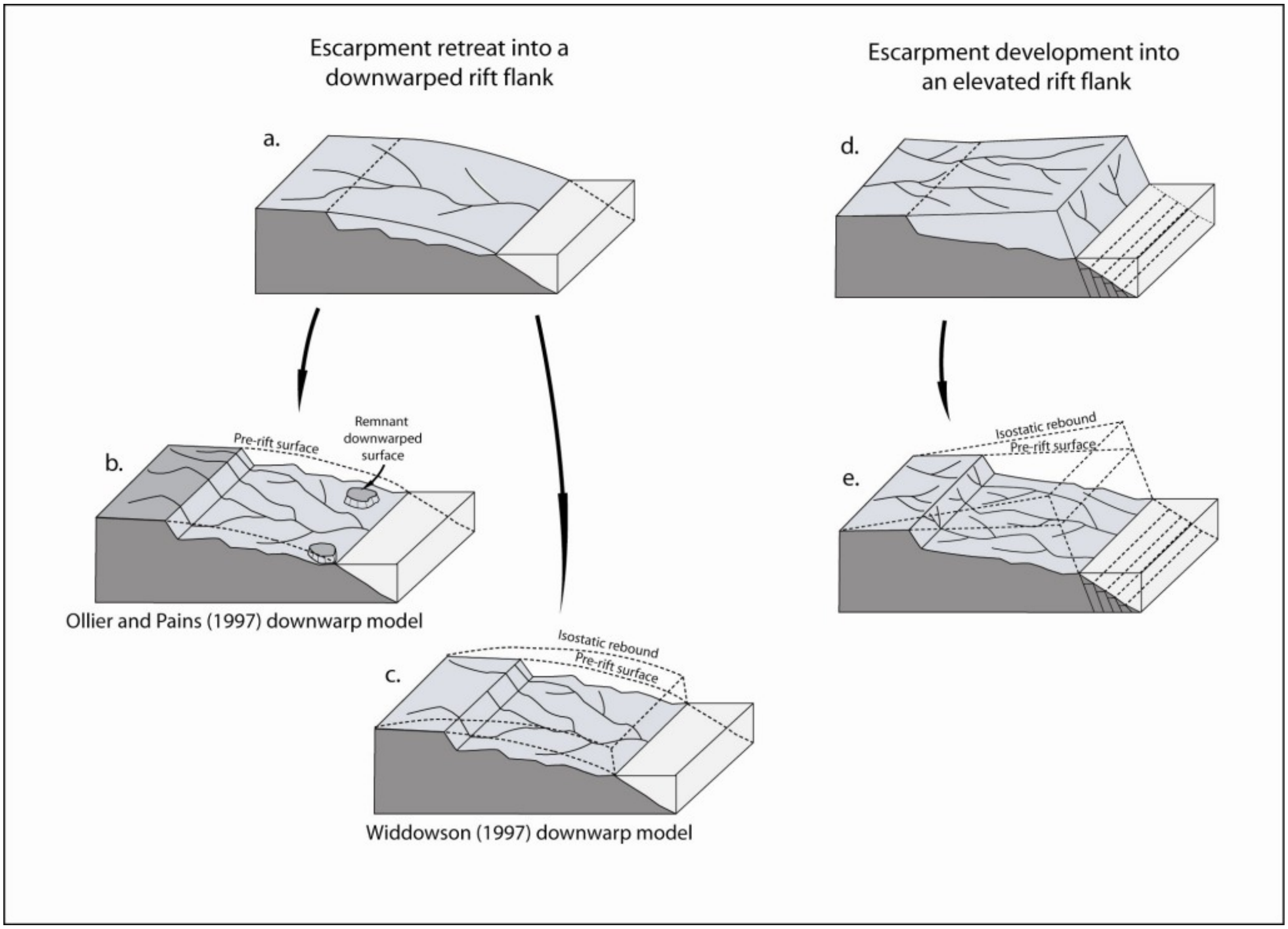

Figure 1 Conceptual models of elevated passive margin development. Dashed lines represent missing crustal material. 1a – c: Escarpment retreat into a downwarped rift flank. Note the small volume of the crustal prism removed and the presence of coastal facets in b. The Widdowson (1997) downwarp model (c) incorporates downwarp geometry but also includes isostatic rebound. Escarpment development into an elevated rift flank (d and e). Note the large volume of the crustal prism removed (with accompanying isostatic rebound)

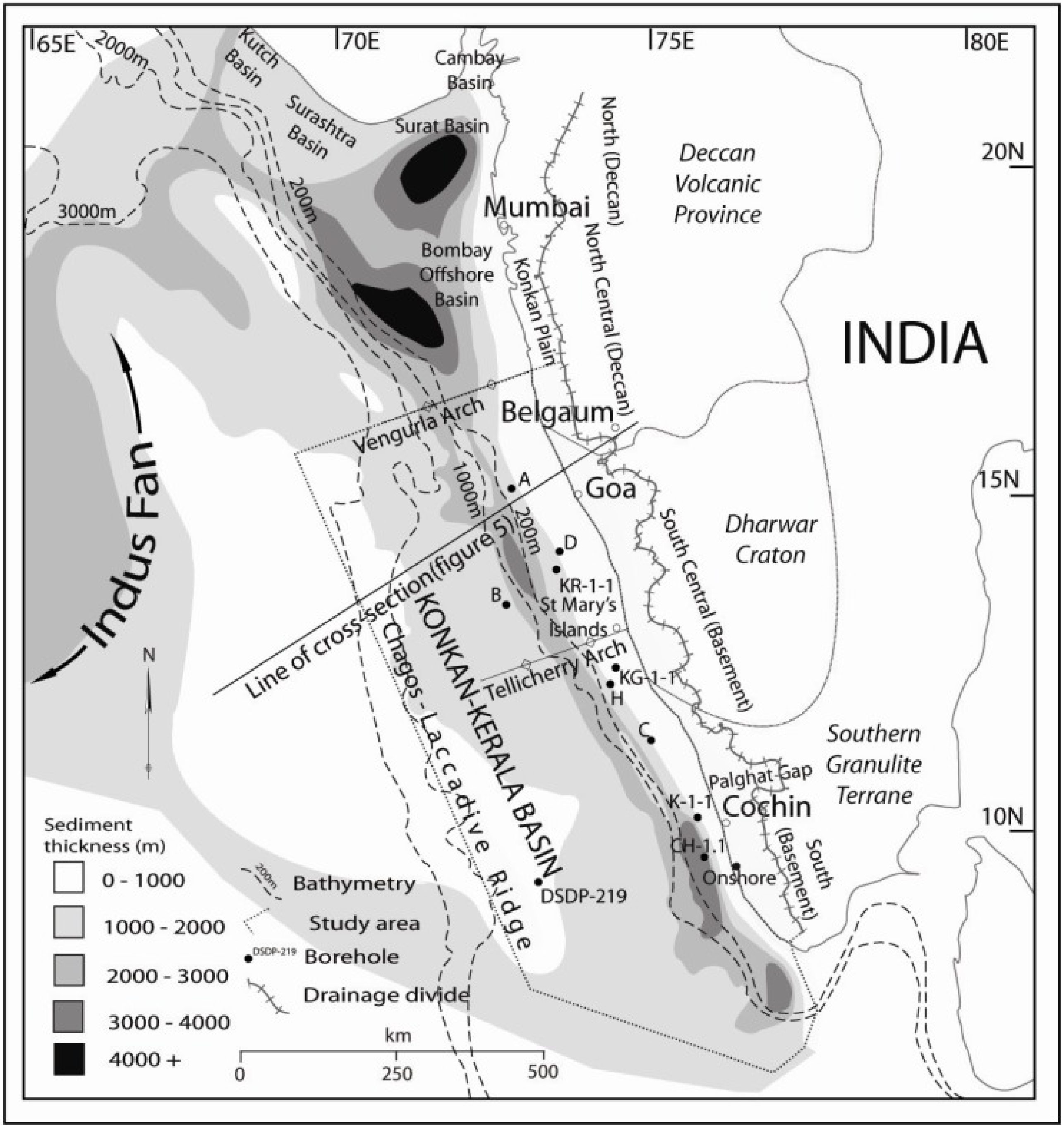

Figure 2 Western India, the Konkan-Kerala basin and surrounding area. Total sediment thickness maps of the offshore basins are compiled from data given by Rao & Srivastava (1984) and Rao *et al*., (2002). Also shown are the locations of wells used in the study and the location of the seismic profile of Chaubey *et al*. (2002). DEM-derived contours onshore, the regional watershed and the area used for mass-balance calculations are also shown.

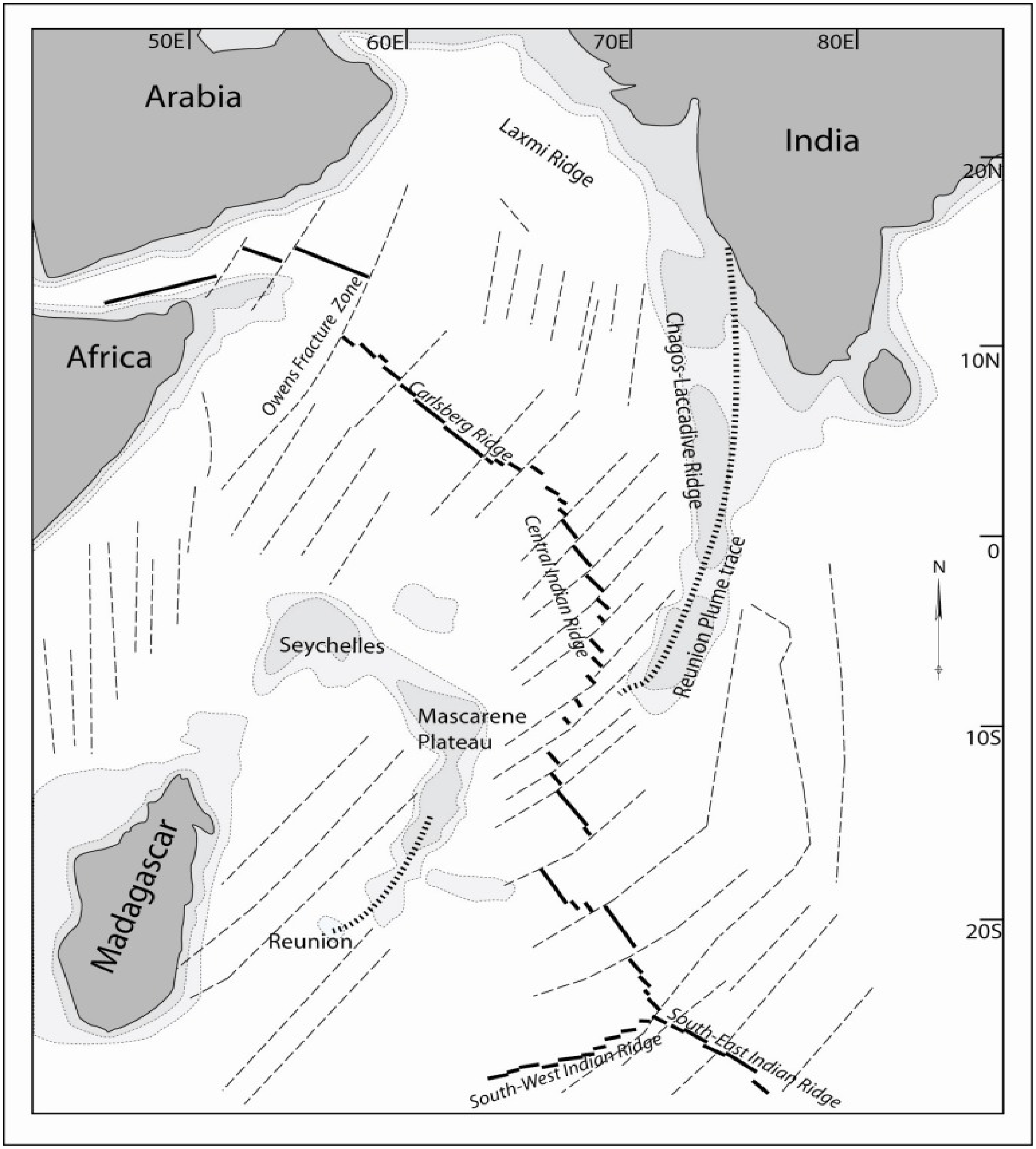

Figure 3 Tectonic map of the Indian Ocean displaying: major spreading centres (solid lines), major transform faults (narrow dashed lines) and the north-south trace of the Reunion Plume (wide dashed line).

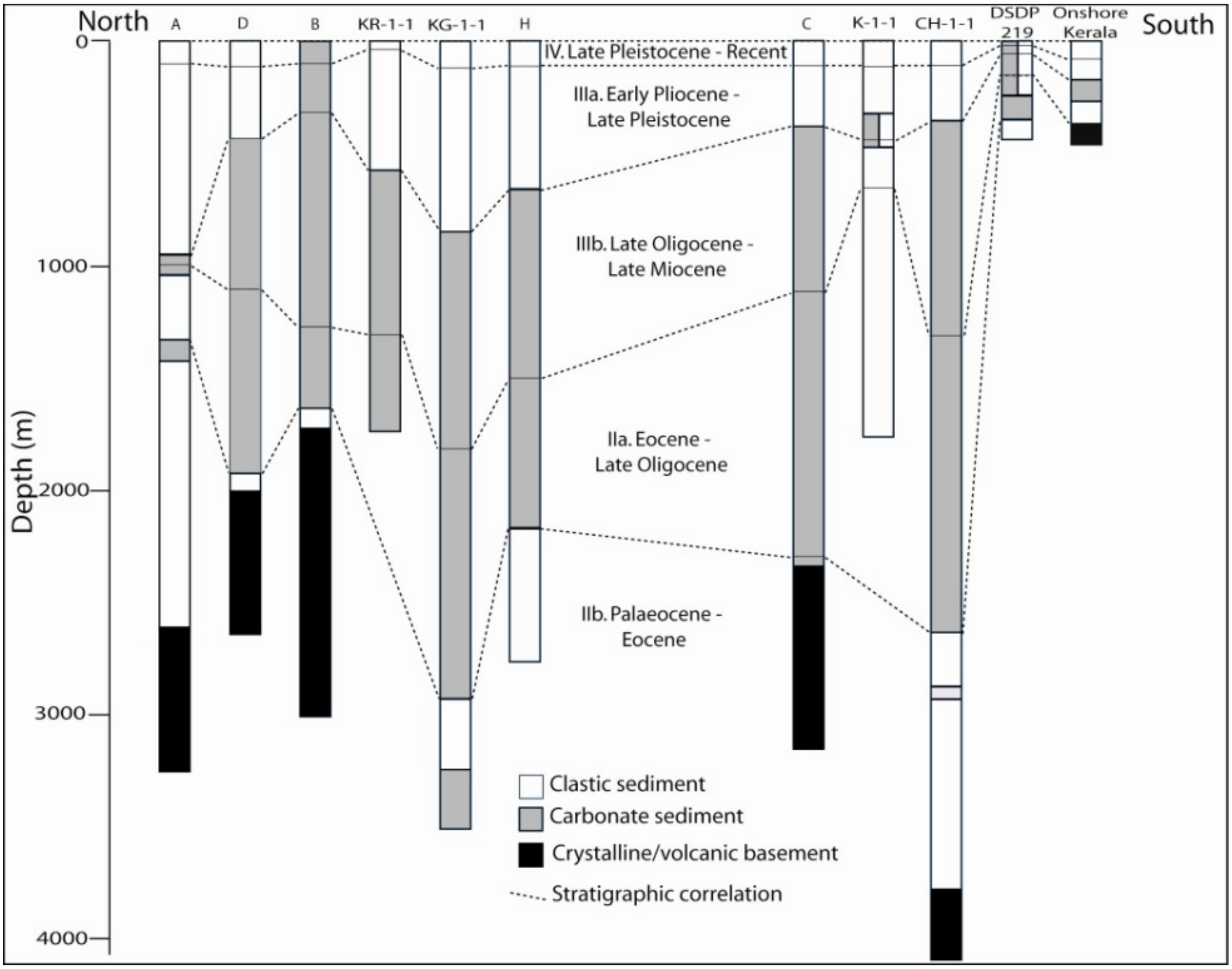

Figure 4 Simplified lithologies and startigraphies of wells in the Konkan Kerala Basin. The dashed lines are stratigraphic correlations for the five sub-sequences used in the study. Wells A, B, C, D, H from Rao *et al*. (2002); K-R-1 and DSDP 219 from Chaubey *et al*., (2002); K-1-1 and CH-1-1 from Singh & Lal (1993); KG-1-1 and onshore Kerala from Gunell & Radhakrishna (2001).

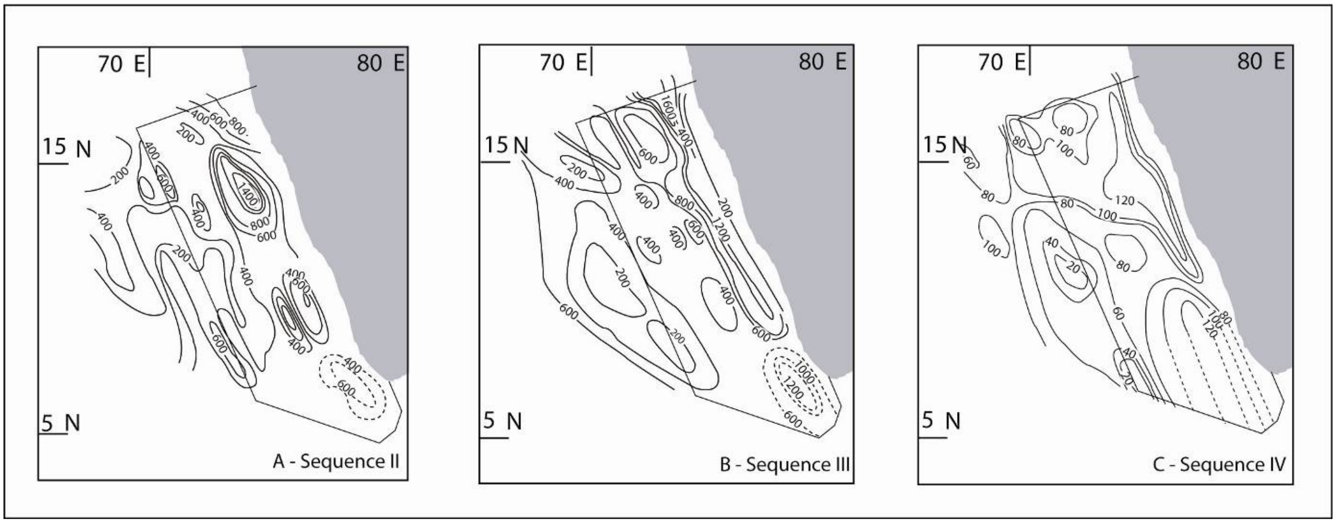

Figure 5 Sediment-thickness maps of the three broad sequences discussed in the text (modified after Rao & Srivastava, 1984). The broken lines are extrapolations based on the total sediment thickness data. Units are two way travel time.

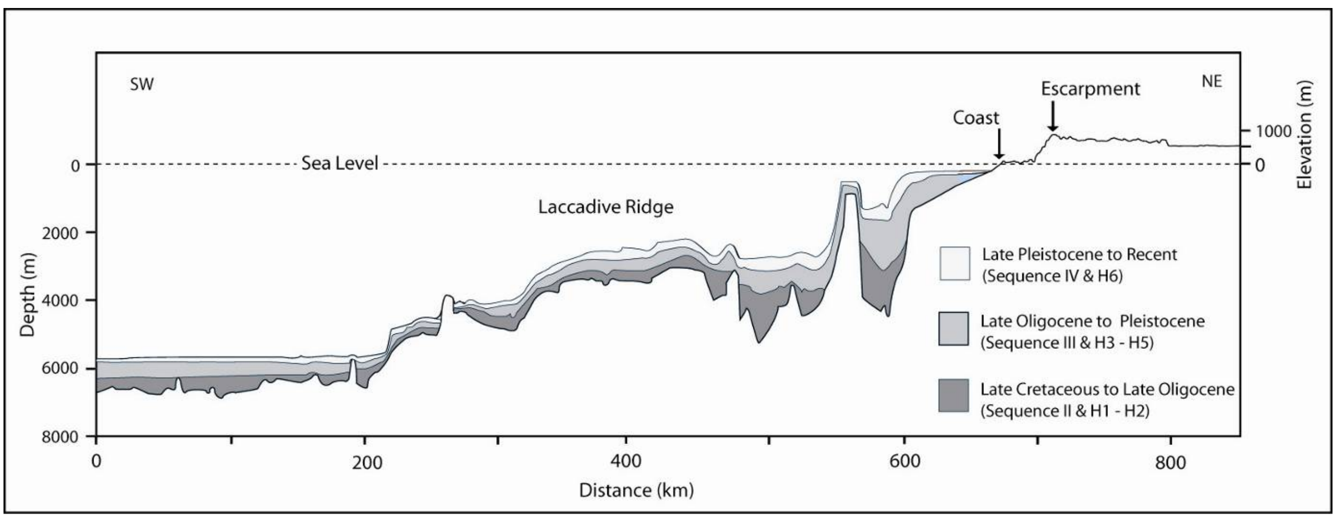

Figure 6 Generalized cross section along the northern part of the Konkan Kerala Basin (based on the seismic profile of Chaubey *et al*., (2002) showing the major lithostratigraphic units, and the topographic profile onshore. Vertical exaggeration = 25x

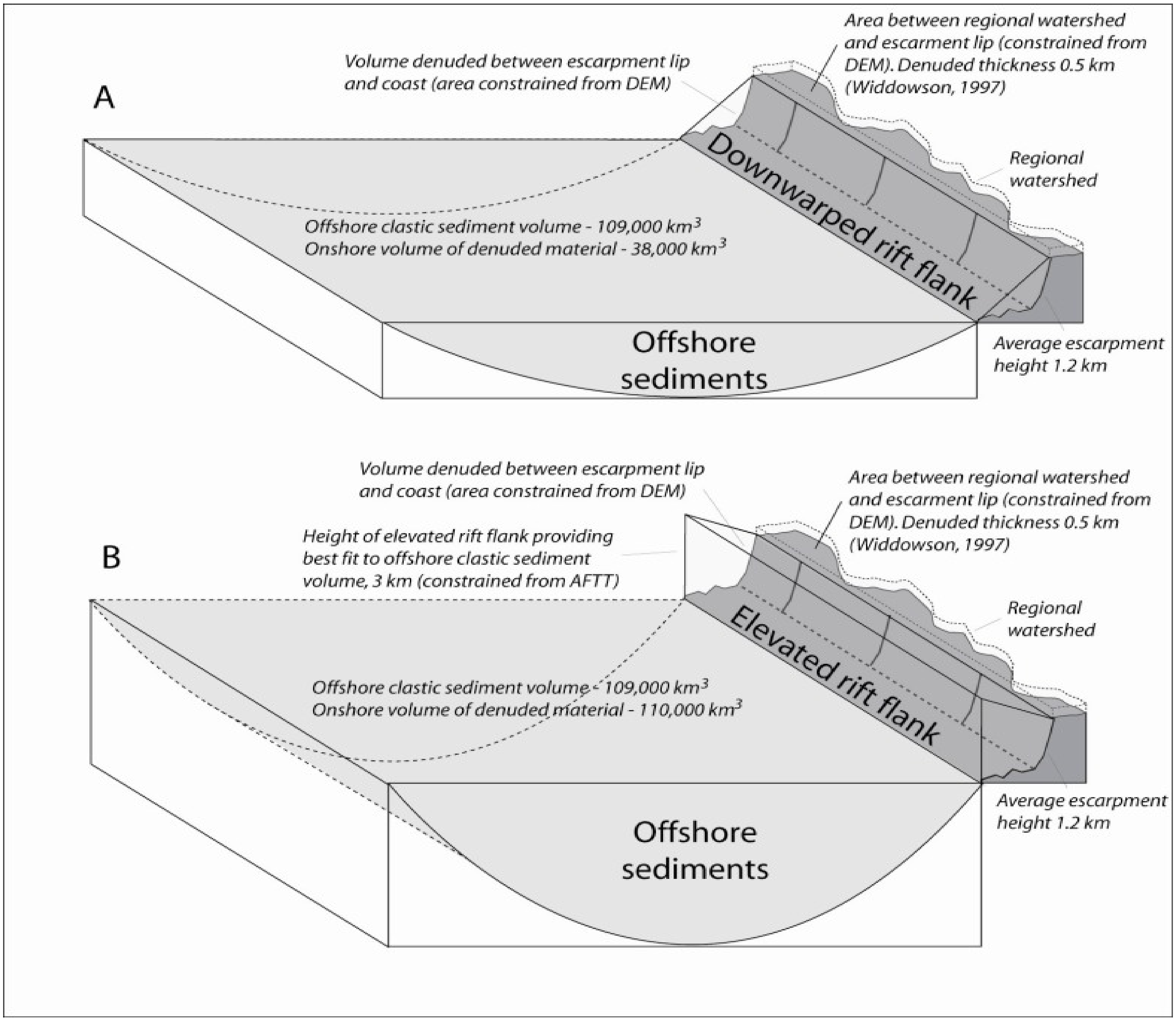

Figure 7 Diagrammatic representation of the mass balance procedure. Different onshore denuded prisms produce different volumes. The form of the crustal prism depends on both the pre-rift palaeoelvation and the flexural response of the lithosphere. A wedged-shaped prism thinning to the coast characterises Ollier and Pains (1997) downwarped rift shoulder (A), and an inverted wedge-shaped prism of eroded crust characterises an elevated rift shoulder with denudational isostasy accompanying its denudation (B). The onshore denuded material is a combination of the denuded prisms and the denuded material between the escarpment lip and the regional watershed (see text for details). The onshore volume of denuded material is then compared to the volume of clastic material present offshore.

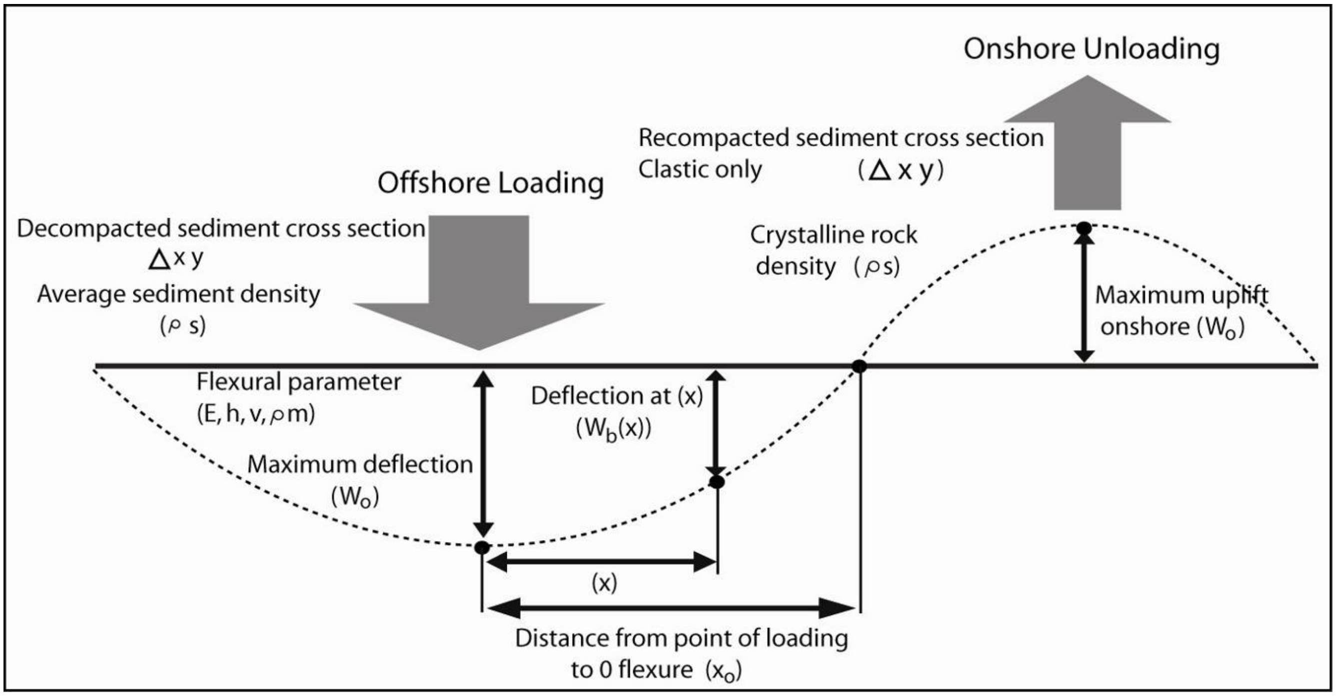

Figure 8 Schematic diagram of an idealized section of crust represented as an infinitely long, thin, elastic plate overlying a fluid and the terms used in eq. 2 – 7.

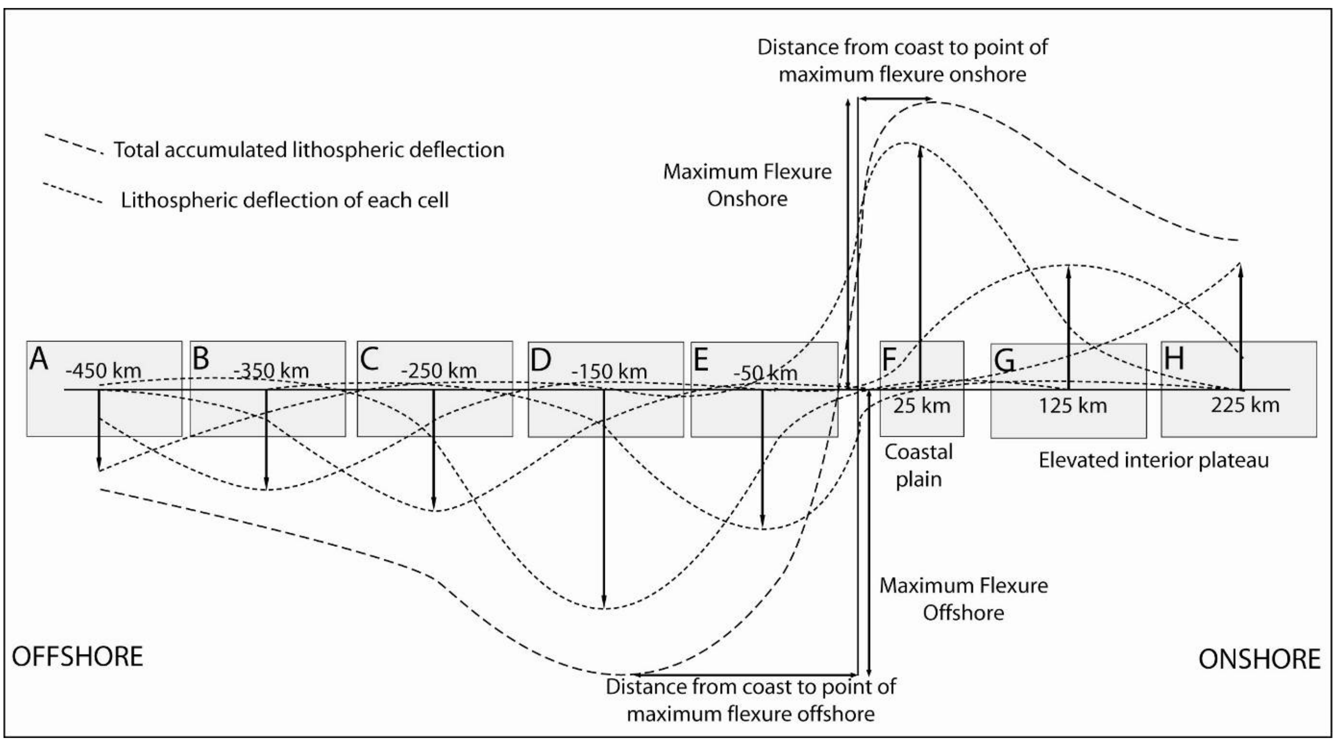

Figure 9. Schematic diagram of the model used to simulate flexural isostasy for Western India. The plate is loaded by sedimentation in cells A to E and unloaded by denudation in cells F to H. The amount of deflection provided by the cells (thin dashed lines) depends on their cross sectional area, sediment density and position. The total accumulated deflection is represented by the thick dashed line.

The position and maximum magnitude of flexure both onshore and offshore are reported in Tables 4 and 5.

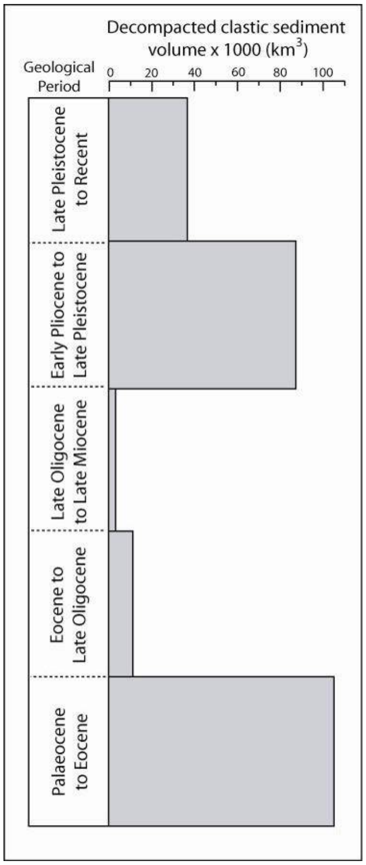

Figure 10 Results of the sediment analysis. The grey bars are the decompacted clastic sediment volumes for each of the five sub-sequences.

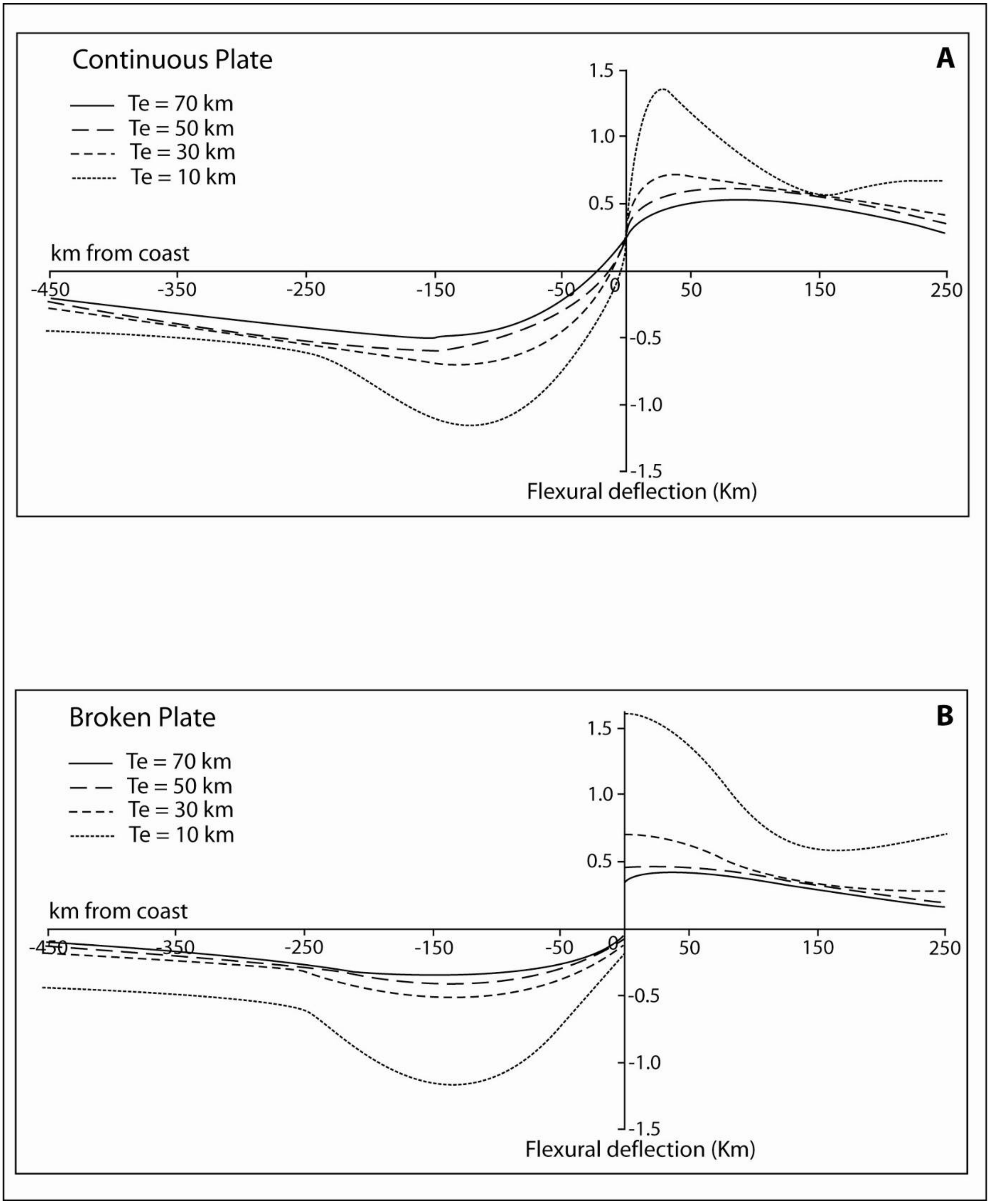

Figure 11 Total accumulated flexure for different values of effective elastic thickness for a continuous plate (A) and a broken plate (B) across Western India (modelled as a thin plate).

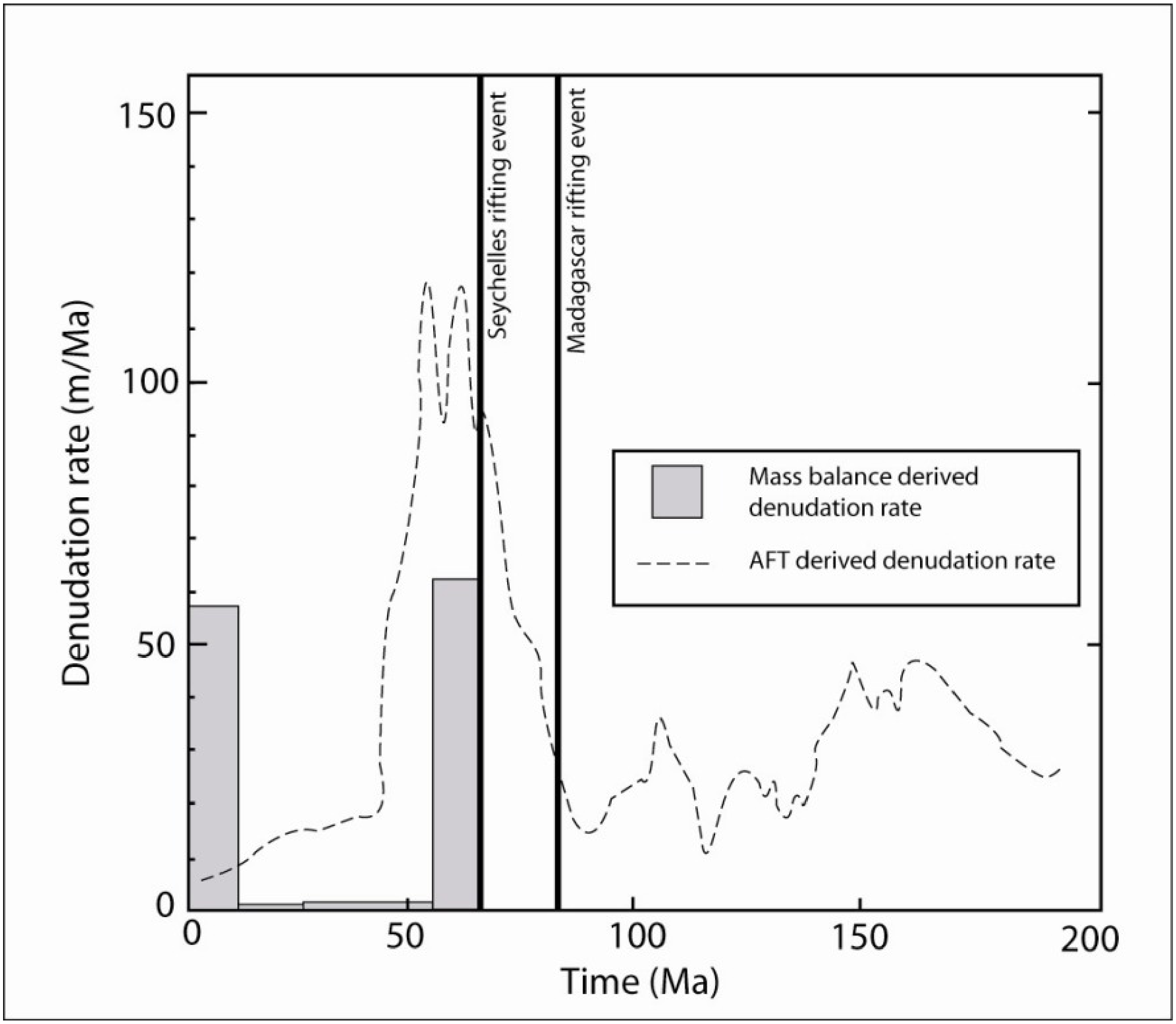

Figure 12 Mesozoic and Cenozoic denudation rates constrained from AFTT (dashed line) (Gunnell *et al.*, 2003) and Cenozoic denudation rates constrained from the mass balance analysis (grey bars). The mass balance analysis highlights two increases in denudation, one phase at the beginning of the Cenozoic and a second younger phase in the Pliocene. The AFT data record an increase in denudation in the earlier Palaeocene phase but not the later, post-Miocene phase. Madagascar rifted at ca. 88 Ma (Storey *et al*, 1995) and the Seychelles rifted at ca. 65 Ma (McKenzie and Sclater, 1971; Naini and Talwani, 1983; Norton and Sclater, 1979; Schlich, 1982).